



**UNIVERSIDAD DE INVESTIGACIÓN DE
TECNOLOGÍA EXPERIMENTAL YACHAY**

Escuela de Ciencias Biológicas e Ingeniería

**TÍTULO: Synthesis and characterization of *in vitro* biologically
active protein-polymer-based nanoparticulate formulations**

Trabajo de integración curricular presentado como requisito para la
obtención del título de Ingeniero Biomédico

Autor:

Gancino Guevara Marlon Alexander

Tutor:

Ph.D. Santiago Vispo Nelson

Cotutores:

Ph.D. Pedroso Santana Seidy

Ph.D. Fleitas Salazar Noralvis

Urcuquí, febrero 2020.

Urucuquí, 28 de febrero de 2020

SECRETARÍA GENERAL
(Vicerrectorado Académico/Cancillería)
ESCUELA DE CIENCIAS BIOLÓGICAS E INGENIERÍA
CARRERA DE BIOMEDICINA
ACTA DE DEFENSA No. UI TEY-BIO-2020-00005-AD

En la ciudad de San Miguel de Urucuquí, Provincia de Imbabura, a los 28 días del mes de febrero de 2020, a las 15:30 horas, en el Aula CHA-01 de la Universidad de Investigación de Tecnología Experimental Yachay y ante el Tribunal Calificador, integrado por los docentes:

Presidente Tribunal de Defensa	<u>Dr. DAHOUMANE , SI AMAR , Ph.D.</u>
Miembro No Tutor	<u>Dr. ALEXIS FRANK , Ph.D.</u>
Tutor	<u>Dr. SANTIAGO VISPO, NELSON FRANCISCO , Ph.D.</u>

Se presenta el(la) señor(ita) estudiante **GANCINO GUEVARA, MARLON ALEXANDER**, con cédula de identidad No. 1724735558, de la ESCUELA DE CIENCIAS BIOLÓGICAS E INGENIERÍA, de la Carrera de BIOMEDICINA, aprobada por el Consejo de Educación Superior (CES), mediante Resolución RPC-SO-43-No.496-2014, con el objeto de rendir la sustentación de su trabajo de titulación denominado: **Synthesis and characterization of in vitro biologically active protein-polymer-based nanoparticulate formulations**, previa a la obtención del título de INGENIERO/A BIOMÉDICO/A.

El citado trabajo de titulación, fue debidamente aprobado por el(los) docente(s):

Tutor Dr. SANTIAGO VISPO, NELSON FRANCISCO , Ph.D.

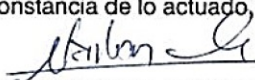
Y recibió las observaciones de los otros miembros del Tribunal Calificador, las mismas que han sido incorporadas por el(la) estudiante.

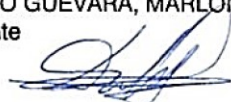
Previamente cumplidos los requisitos legales y reglamentarios, el trabajo de titulación fue sustentado por el(la) estudiante y examinado por los miembros del Tribunal Calificador. Escuchada la sustentación del trabajo de titulación, que integró la exposición de el(la) estudiante sobre el contenido de la misma y las preguntas formuladas por los miembros del Tribunal, se califica la sustentación del trabajo de titulación con las siguientes calificaciones:

Tipo	Docente	Calificación
Miembro Tribunal De Defensa	Dr. ALEXIS FRANK , Ph.D.	10.0
Tutor	Dr. SANTIAGO VISPO, NELSON FRANCISCO , Ph.D.	10.0
Presidente Tribunal De Defensa	Dr. DAHOUMANE , SI AMAR , Ph.D.	10.0

Lo que da un promedio de: **10 (Diez punto Cero)**, sobre 10 (diez), equivalente a: **APROBADO**

Para constancia de lo actuado, firman los miembros del Tribunal Calificador, el/la estudiante y el/la secretario ad-hoc.

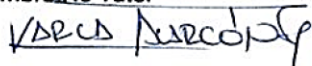

GANCINO GUEVARA, MARLON ALEXANDER
Estudiante


Dr. DAHOUMANE , SI AMAR , Ph.D.
Presidente Tribunal de Defensa


Dr. SANTIAGO VISPO, NELSON FRANCISCO , Ph.D.
Tutor



Dr. ALEXIS FRANK, Ph.D.
Miembro No Tutor



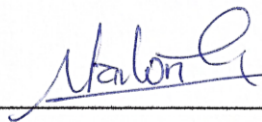
ALARCON FELIX, KARLA ESTEFANIA
Secretario Ad-hoc



AUTORÍA

Yo, **Marlon Alexander Gancino Guevara**, con cédula de identidad 1724735558, declaro que las ideas, juicios, valoraciones, interpretaciones, consultas bibliográficas, definiciones y conceptualizaciones expuestas en el presente trabajo; así como, los procedimientos y herramientas utilizadas en la investigación, son de absoluta responsabilidad del autor del trabajo de integración curricular. Así mismo, me acojo a los reglamentos internos de la Universidad de Investigación de Tecnología Experimental Yachay.

Urcuquí, febrero 2020.



Marlon Alexander Gancino Guevara

CI: 1724735558

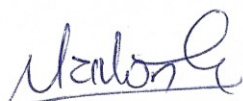
AUTORIZACIÓN DE PUBLICACIÓN

Yo, **Marlon Alexander Gancino Guevara**, con cédula de identidad 1724735558, ratifico que el presente trabajo de investigación es parte de un proyecto de I+D que aún se encuentra en curso, cuya propiedad intelectual pertenece a la Universidad de Concepción, Chile.

Expongo a su vez que no está en mi poder legal el ceder a la Universidad Yachay Tech el derecho de publicación de la presenta obra o el reconocimiento económico por este concepto. Declaro además que el texto del presente trabajo de titulación no podrá ser cedido a ninguna empresa editorial para su publicación u otros fines, sin contar previamente con la autorización escrita de la Universidad de Concepción.

Asimismo, autorizo a la Universidad que realice la digitalización y publicación de este trabajo de integración curricular en el repositorio virtual, de conformidad a lo dispuesto en el Art. 144 de la Ley Orgánica de Educación Superior.

Urcuquí, febrero 2020.



Marlon Alexander Gancino Guevara

CI: 1724735558

Dedicatoria

Dedico este trabajo a:

A Dios. Su amor siempre me ha guiado y me ha permitido tener una vida muy bonita.

Al sueño que motivó la creación de la Universidad Yachay Tech. Enamorarnos del conocimiento nos permitirá vencer a la ignorancia, injusticia, corrupción, e inequidad.

Al trabajo incansable de mis profesores. Avanzo sobre hombros de gigantes.

Al amor de mi familia. Siempre me han apoyado y confiado en mí.

Finalmente, a mis perritas que, aunque no tengan idea qué significa nanomedicina y nunca se lleguen a enterar que las nombré aquí, me alegran la vida.

Marlon Alexander Gancino Guevara

Agradecimientos

Este manuscrito es el resultado de aproximadamente cinco años y medio de experiencias gratificantes que siempre recordaré con aprecio.

Este proyecto se estructuró en dos etapas: una etapa conceptual y otra experimental. Agradezco a la Universidad Yachay Tech, en especial a la Escuela de Ciencias Biológicas e Ingeniería y a la Escuela de Ciencias Químicas e Ingeniería por proporcionarme todas las herramientas que necesité para desarrollar la etapa conceptual de mi investigación.

Agradezco principalmente a mi tutor Ph.D. Nelson Santiago Vispo por haberme confiado este proyecto, por haberme guiado excepcionalmente en la conceptualización de la investigación, por motivarme durante el desarrollo de este trabajo, por convertirse en un buen amigo, por prepararme, y por vincularme con la Universidad de Concepción; en donde llevé a cabo la etapa experimental de mi tesis.

Agradezco a Ph.D. Jorge Toledo por permitirme formar parte del Laboratorio de Biotecnología y Biofármacos de la Universidad de Concepción y apoyarme durante el tiempo que duró mi estancia. Agradezco a todo el equipo de investigadores de este laboratorio por recibirme con amabilidad, y por las mañanas, tardes, y noches de café.

Agradezco con mucho aprecio a mis cotutores, mentores, y amigos, Ph.D. Seidy Pedroso y Ph.D. Noralvis Fleitas por permitirme formar parte de su investigación, por acompañarme con sus consejos todo este tiempo, por su paciencia, por darme ánimos, y por las incontables buenas conversaciones. Gracias a ellos pude desarrollarme en el laboratorio, completar la parte experimental de mi tesis, y obtener resultados excelentes.

Agradezco a los miembros de mi tribunal de defensa Ph.D. Si Amar Dahoumane y Ph.D. Frank Alexis por sus comentarios y aportes a este manuscrito, y por haber sido, conjuntamente con Ph.D. Ming Ni, los profesores que despertaron mi interés por la nanomedicina.

Por otro lado, agradezco infinitamente a mi familia por siempre estar conmigo y quererme tanto. Gracias a todos ellos sé que este es el inicio de todo y que llegaré demasiado lejos.

Estos cinco años y medio nunca hubieran sido tan gratificantes y tan llenos de buenas experiencias sin mis amigos. Su compañía y los momentos que vivimos no tienen precio. A todos ustedes, ¡gracias!

Por último y con todo mi corazón, May te agradezco por acompañarme con tus ojitos bonitos, escucharme, y aconsejarme todo este tiempo; también, te agradezco por haberme enseñado a ser más organizado y a ser una mejor persona.

Marlon Alexander Gancino Guevara

Resumen

La terapéutica con proteínas se considera una estrategia atractiva y valiosa para el tratamiento de una extensa lista de enfermedades difíciles de medicar. Sin embargo, su efectividad clínica se ve disminuida por su alta labilidad en entornos fisiológicos. En particular, el interferón α (IFN α) es un agente terapéutico utilizado en medicina humana y veterinaria para combatir infecciones virales y numerosos tipos de cáncer. No obstante, su rendimiento farmacológico está limitado por su degradación y la eliminación rápida de la circulación sistémica en el sistema reticuloendotelial (RES). Esta tesis de pregrado presenta una estrategia novedosa para la optimización farmacológica de formulaciones de IFN α a través del uso de nanopartículas poliméricas biocompatibles y biodegradables. El trabajo describe el diseño, síntesis y caracterización de una formulación de pIFN α en nanopartículas de quitosano (CS NPs). Nanopartículas esféricas de quitosano cargadas con rpIFN α (rpIFN α -loaded CS NPs) con un diámetro hidrodinámico promedio, índice de polidispersidad y potencial zeta igual a 196.82 nm, 0.22, y +30.04 mV, respectivamente, fueron sintetizadas reproduciblemente mediante gelificación ionotrópica entre quitosano y tripolifosfato de sodio (TPP). Los ensayos de encapsulación de proteínas demostraron que las CS NPs podían encapsular eficientemente BSA conjugado con FITC ((FITC) BSA) y rpIFN α . Específicamente, la eficiencia de encapsulación (EE%) de 250 μ g de rpIFN α fue igual al 75%. Por otro lado, los estudios *in vitro* de la cinética de liberación de proteínas mostraron que rpIFN α se descargaba sostenidamente de las CS NPs durante 171 horas. Los ensayos *in vitro* de viabilidad celular MTT demostraron que las CS NPs y las rpIFN α -loaded CS NPs eran biocompatibles para las células de riñón porcino-15 (PK-15). La captación celular de (FITC)BSA-loaded CS NPs fue confirmada en células de epitelio humano tipo 2 (HEp-2) usando microscopía confocal. Finalmente, los ensayos *in vitro* de actividad biológica de proteínas encontraron que el rpIFN α liberado de las CS NPs retenía una actividad antiviral mayor de 10^3 UI en HEp-2 contra Mengovirus, durante al menos 120 horas. En conclusión, estos resultados son alentadores y sugieren que las rpIFN α -cargado CS NPs podrían utilizarse para diseñar formulaciones de pIFN α con un rendimiento farmacológico optimizado *in vivo* para fines veterinarios.

Palabras Clave: Terapéutica de proteínas, administración de proteínas, formulación de proteínas, interferón α porcino recombinante, nanopartículas de quitosano, gelificación ionotrópica, actividad antiviral.

Abstract

Protein therapeutics is considered as an attractive and valuable strategy for treating an extensive list of difficult-to-treat diseases. However, its clinical effectiveness is diminished by the high lability of proteins in physiological environments. In particular, interferon α (IFN α) is a therapeutic agent used in human and veterinary medicine to address viral infections and numerous types of cancer. Nevertheless, its pharmacological performance is limited by its degradation and rapid clearance from the systemic circulation by the reticuloendothelial system (RES). This undergraduate thesis presents a novel strategy for the pharmacological optimization of IFN α formulations by using biocompatible and biodegradable polymer-based nanoparticles. This work describes the design, synthesis, and characterization of a chitosan-based nanoparticulate formulation of recombinant porcine IFN α (rpIFN α). Spherical rpIFN α -loaded chitosan nanoparticles (rpIFN α -loaded CS NPs) with an average hydrodynamic diameter, polydispersity index, and zeta potential equal to 196.82 nm, 0.22, and +30.04 mV, respectively, were reproducibly synthesized by ionotropic gelation between chitosan and sodium tripolyphosphate (TPP). Protein encapsulation assays proved that CS NPs could efficiently encapsulate FITC-conjugated BSA ((FITC)BSA) and rpIFN α . Specifically, encapsulation efficiency (EE%) of 250 μ g of rpIFN α was equal to 75%. On the other hand, *in vitro* protein release kinetics studies showed a sustained release of rpIFN α from the CS NPs for 171 h. MTT *in vitro* cell viability assays demonstrated that CS NPs and rpIFN α -loaded CS NPs were biocompatible to porcine kidney-15 (PK-15) cells. Cellular uptake of (FITC)BSA-loaded CS NPs was confirmed in human epithelial type 2 (HEp-2) cells using confocal microscopy. Finally, *in vitro* protein biological activity assays found that rpIFN α released from CS NPs retained an antiviral activity greater than 10^3 IU in HEp-2 against Mengovirus, for at least 120 h. In conclusion, these results are encouraging and suggest that rpIFN α -loaded CS NPs could be used for designing pIFN α formulations with optimized *in vivo* pharmacological performance in veterinary purposes.

Keywords: Protein therapeutics, protein delivery, protein formulation, recombinant porcine interferon α , chitosan nanoparticles, ionotropic gelation, antiviral activity.

Content

Resumen	VIII
Abstract.....	IX
List of Figures	XIII
List of Tables	XIV
1. Introduction.....	1
2. Hypothesis.....	4
3. General Objective	4
4. Specific Objectives	4
5. Literature Review	6
5.1. Nanomedicine-based drug delivery systems.....	6
5.2. Polymer-based nanoparticles as drug delivery systems	7
5.3. Physicochemical and biological considerations for polymer-based nanoparticles used in drug delivery applications.....	8
5.3.1. Nanoparticle size, size distribution and morphology.....	9
5.3.2. Nanoparticle composition	10
5.3.3. Nanoparticle surface charge.....	10
5.3.4. Drug loading and release	12
5.3.5. Polymer-based nanoparticles and cell viability.....	13
5.3.6. Cellular uptake	14
5.4. Chitosan nanoparticles as protein delivery systems.....	14
5.4.1. Chitosan nanoparticles by ionotropic gelation.....	16
5.5. Porcine IFN α therapeutics	18
6. Materials and Methods.....	22
6.1. Materials.....	22
6.2. Methods.....	22
6.2.1. Conjugation of Bovine Serum Albumin with Fluorescein Isothiocyanate	22
6.2.2. Synthesis of chitosan nanoparticles and protein-loaded chitosan nanoparticles	22

6.2.3.	Nanoparticles characterization	23
6.2.3.1.	Hydrodynamic diameter, polydispersity index, and zeta potential	23
6.2.3.2.	Morphology	23
6.2.3.3.	Infrared spectroscopy	23
6.2.3.4.	Fluorescence spectroscopy	24
6.2.3.5.	Encapsulation efficiency of rpIFN α	24
6.2.3.6.	In vitro protein release studies	24
6.2.4.	Experiments with cancer cell lines	25
6.2.4.1.	Cytotoxicity assay	25
6.2.4.2.	Cellular uptake of (FITC)BSA-loaded CS NPs	25
6.2.4.3.	<i>In vitro</i> biological activity of the encapsulated rpIFN α	26
6.2.5.	Statistics	26
7.	Results and Discussion	28
7.1.	Synthesis of chitosan nanoparticles	28
7.1.1.	Standardization of chitosan nanoparticles synthesis	28
7.1.2.	Reproducibility of the chitosan nanoparticle synthesis reaction	30
7.1.3.	Physical stability characterization	30
7.1.4.	Structural characterization	31
7.1.5.	Morphology characterization	32
7.1.6.	Scaling of chitosan nanoparticle synthesis reaction	33
7.2.	Synthesis of protein-loaded chitosan nanoparticles	34
7.2.1.	Protein encapsulation	34
7.2.2.	Encapsulation of recombinant porcine IFN α protein	35
7.2.2.1.	Size and size distribution characterization	35
7.2.2.2.	Physical stability characterization	36
7.2.2.3.	Morphology characterization	37
7.2.2.4.	In Vitro drug release kinetics profile	38
7.3.	Cell assays	39
7.3.1.	Cell viability assay	39

7.3.2.	Cellular uptake of protein-loaded chitosan nanoparticles	40
7.3.3.	<i>In vitro</i> antiviral activity of the encapsulated rpIFN α	41
8.	Conclusions and Recommendations	44
	Bibliography	45

List of Figures

1. Illustration of different types of nanoparticles.....	7
2. Representation of polymeric nanoparticles types according to drug encapsulation	7
3. Diagram of electric potential layers of a polymer-based nanoparticle.....	11
4. Methods of drug loading into polymer-based nanoparticles	12
5. Illustration of drug release from the NPs	13
6. Schematics depicting the obtaining of chitosan from the N-deacetylation of chitin.....	15
7. Proposed schematic drawing of CS NPs formation by ionotropic gelation	17
8. Schematic illustration of protein encapsulation in CS NPs by ionotropic gelation	18
9. Molecular structure (ribbon and surface diagram) of IFN α	19
10. DLS characterization of chitosan nanoparticles	30
11. Zeta potential distribution of chitosan nanoparticles	31
12. Normalized ATR-FTIR transmittance spectra of lyophilized chitosan nanoparticles	32
13. Transmission electron micrographs of chitosan nanoparticles	33
14. DLS characterization of CS NPs synthesized by volume-modified formulations.....	34
15. Fluorescence emission spectra of FITC-conjugated BSA and (FITC)BSA-loaded chitosan nanoparticles.....	35
16. DLS characterization of rpIFN α -loaded chitosan nanoparticles.....	36
17. Zeta potential distribution of rpIFN α -loaded chitosan.....	37
18. Transmission electron micrographs of rpIFN α -loaded CS NPs	38
19. Cumulative <i>in vitro</i> protein release profile of chitosan nanoparticles and rpIFN α -loaded chitosan nanoparticles during 171 h.....	39
20. Viability of PK15 cells after the treatment with chitosan nanoparticles and rpIFN α -loaded chitosan nanoparticles	40
21. Confocal micrographs showing the localization of (FITC)BSA-loaded CS NPs in HEp-2 cells	41
22. <i>In vitro</i> antiviral activity of rpIFN α against Mengovirus in Hep-2 cells.....	42

List of Tables

1. Preparative parameters used in the standardization of chitosan nanoparticle synthesis..... 29
2. Standardization results regarding the hydrodynamic diameter and PDI of nanoparticles..... 29
3. ATR-FTIR analysis of chitosan nanoparticles 32

Chapter I

1. Introduction

Protein therapeutics constitutes an attractive and valuable strategy in current medicine to address an extensive list of difficult-to-treat diseases (1). Proteins are endogenous complex molecules which perform highly specific catalytic functions that cannot be mimicked by small-molecule drugs (2). Principal advantages of protein therapeutics include the design and development of novel therapies with enhanced specificity, reduced toxicity, and reduced risk of adverse effects occurrence (3). Despite these advantages, physiological environments diminish the pharmacological performance of proteins (4). Their most critical therapeutic limitations are related to formulation instability, proteolytic degradation, rapid clearance, immunogenicity, low solubility, low intracellular permeability, and, as a consequence, extremely poor bioavailability (5). Nowadays, protein engineering has developed several proteins structural modification-oriented strategies, such as PEGylation, glycosylation, albumin conjugation, or mutations, to surpass those protein therapeutics drawbacks (6); however, in most of the cases the protein biological activity is dramatically affected (3).

In this scenario, the exploitation of drug delivery nanosystems (i.e., nanoparticles) has recently appeared as a sound solution to overcome the above-mentioned limitations without jeopardizing the biological activity of proteins (7,8). To date, the most explored drug delivery nanosystems for protein therapeutics include liposome-, metal oxide-, metal-, and polymer-based nanoparticles (NPs), which are already available for clinical use or in clinical trials (9). Among them, polymer-based nanoparticles (PNPs) have attracted much interest owing to their desirable therapeutic features, such as increased stability, reduced immunogenicity, the ability to overcome biological barriers, the capacity to extend protein half-life and to control protein-delivery (10,11). Chitosan (CS), a natural polymer categorized as "Generally Recognized as Safe" (GRAS) material by the Food and Drug Administration (FDA) of the United States of America (12), is among the most commonly used polymers for nanoparticle assembling (13). Valuable properties of chitosan, such as hydrophilicity, high biocompatibility, biodegradability, good permeability, and non-antigenicity, justify its extensive use (14). Besides, CS possesses advantageous physicochemical properties that enable the synthesis of NPs in mild conditions, avoiding toxic reagents, while obtaining high protein encapsulation efficiency (EE%) results (15).

Interferon α (IFN α) is an immunomodulatory protein with antiviral and antiproliferative properties, present in all mammalian species (16). IFN α therapeutics has an outstanding relevance in

both human and veterinary medicine; being used for the treatment of several diseases including viral infections and various types of cancer (e.g., hairy cell leukemia, AIDS-related Kaposi's sarcoma, follicular non-Hodgkin's, lymphoma, or renal cell carcinoma) (17,18). In particular, the immunoadjuvant and the antiviral activity of porcine interferon α (pIFN α) have been widely reported (19,20), highlighting its importance for the development of the global pig industry (20–22).

While IFN α possesses tremendous potential as an antiviral, immunomodulatory, and anticancer drug, its therapeutic effect is limited due to the degradation and rapid clearance from the systemic circulation by the reticuloendothelial system (RES) (23). As a result, high doses of IFN α formulations have to be administered in frequent regimes to attain its therapeutic window (24). Consequently, this is associated with harsh dose-dependent adverse effects, such as immunogenic reactions (25). The gold-standard approach for extending protein half-life is the use of PEGylated IFN α (PEG-IFN α) (26); however, as mentioned above, PEGylation reduces the biological activity of IFN α in comparison with its unmodified counterpart (26,27).

Nowadays, numerous drug delivery nanosystems have been proposed as nanocarriers for IFN α therapeutics (23–25). Indeed, two polymer-based nanoformulations for IFN α therapeutics, brand-named Pegasys® (Genentech, U.S.) and PegIntron® (Merck, U.S.), are currently available for clinical use (9,28). In both cases, PEGylated human IFN α (PEG-hIFN α) has been encapsulated (9). However, since most of the efforts orient to the development of human-directed IFN α therapeutics, few veterinary-purposed polymer-based nanoformulations of IFN α have been, so far, described in the literature (24).

In this context, the present work aims at designing, synthesizing, characterizing, and evaluating the biological activity of a novel nanoformulation of recombinant porcine interferon α (rpIFN α) loaded within CS NPs (rpIFN α -loaded CS NPs). First, this work focuses on the synthesis of protein-delivery CS nanosystems by ionotropic gelation between polyanionic sodium tripolyphosphate (TPP) and low molecular weight chitosan. Second, the study pursues the encapsulation of BSA as a model protein, and rpIFN α as the therapeutic protein of interest. Finally, this investigation purposes the quantification of nanoencapsulated rpIFN α biological activity by evaluating its antiviral activity *in vitro*.

Chapter II

2. Hypothesis

In vitro biologically active protein nanoparticle-based formulations can be obtained by ionotropic gelation with chitosan and sodium tripolyphosphate.

3. General Objective

To synthesize biocompatible and biodegradable protein-loaded nanoparticles, which preserve *in vitro* protein biological activity

4. Specific Objectives

- i. To standardize and perform protein nanoencapsulation reactions using ionotropic gelation method.
- ii. To characterize the nanoparticles according to size, physical stability, morphology, chemical composition, drug encapsulation efficiency, *in vitro* protein release kinetics, *in vitro* cellular uptake, and *in vitro* cytotoxicity.
- iii. To evaluate the conservation of the biological activity of the nanoencapsulated proteins by *in vitro* activity assays.

Chapter III

5. Literature Review

5.1. Nanomedicine-based drug delivery systems

Nanomedicine is a cutting-edge technology generally understood as the incorporation of nanotechnology in medicine-purposed sciences (29,30). It aims at the development of novel therapeutic systems for diagnosis, sensing, imaging, and therapy (30,31). Until now, nanomedicine has been mainly exploited for enhancing relevant medical fields, such as drug delivery, *in vitro* and *in vivo* diagnostics, drug discovery, and *in vivo* imaging (32,33). Among the nanomedicine fields, nanomedicine-based drug delivery has been the most widely explored (29,34). Its research is oriented to enhance the pharmacokinetics (PK) and stability of therapeutic agents (e.g., therapeutic biological macromolecules) by improving their delivery and biodistribution using nanostructured carriers (33). Importantly, the principal advantages of nanomedicine-based drug delivery include the design of stable drug formulations with selective targeting, improved solubility and biodistribution, reduced toxicity, enhanced cellular uptake, and controlled drug dosing, while extending drug half-life in blood circulation (7,9).

Nanomedicine-based drug delivery research is broadly supported by the use of nanoparticles (35), which are described as nanoscale (10 – 1000 nm) particles precisely engineered (31,36). NPs are identified as versatile systems that possess unique therapeutic characteristics, including biocompatibility and stability, conferred by their size-related physicochemical properties (e.g., high reactivity) (7). Accordingly, the functionalization of NPs as drug delivery systems by encapsulating or adhering pharmaceutically active ingredients has been receiving much interest (37,38). In complement, NPs have shown the ability to surpass biological barriers and target either passively or actively the tissues (34). As a result, much work on the development of nanoparticles-assisted formulations has been performed to design new therapies (39). Indeed, the literature describes 50 human-oriented nanoparticles-assisted formulations already available for clinical use (e.g., Doxil®, Pegasys®, Macugen®, Infed®, Abraxane®) (9,28). Nevertheless, few studies about drug delivery nanosystems have been published for veterinary use, which provides a lot of room for research (40).

5.2. Polymer-based nanoparticles as drug delivery systems

Nanoparticles can be prepared from many materials, including metals, metal oxides, lipids, and polymers (**Figure 1**) (41). Among them, polymers have attracted an increased interest for the design of drug formulations as drug delivery nanosystems (11,42,43). Pharmacologically, numerous polymers possess several advantages, including the ability to elicit therapeutic responses and form biodegradable and biocompatible platforms for the controlled encapsulation and release of drugs (36,44).

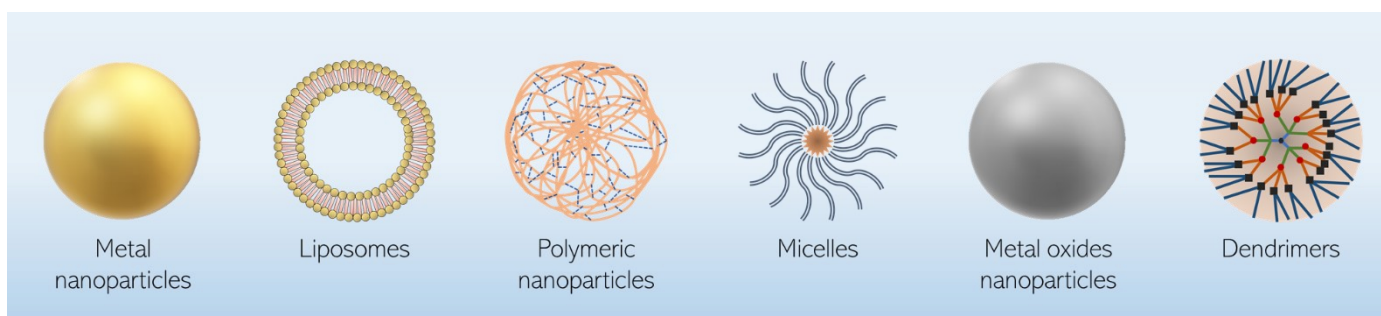


Figure 1. Illustration of different types of nanoparticles.

Polymer-based NPs (PNPs) are defined as solid particles assembled by polymers (e.g., poly(lactic-co-glycolic acid), polylactic acid, alginate, chitosan) (45). According to the way by which the therapeutic agent is encapsulated within the nanoparticles, they can be classified into nanospheres and nanocapsules (43). Thus, nanospheres are described as polymeric matrix nanoparticulated structures inside which a drug is trapped, while nanocapsules are understood as polymeric sheaths surrounding a drug in the nanoparticle core (**Figure 2**) (43,45).

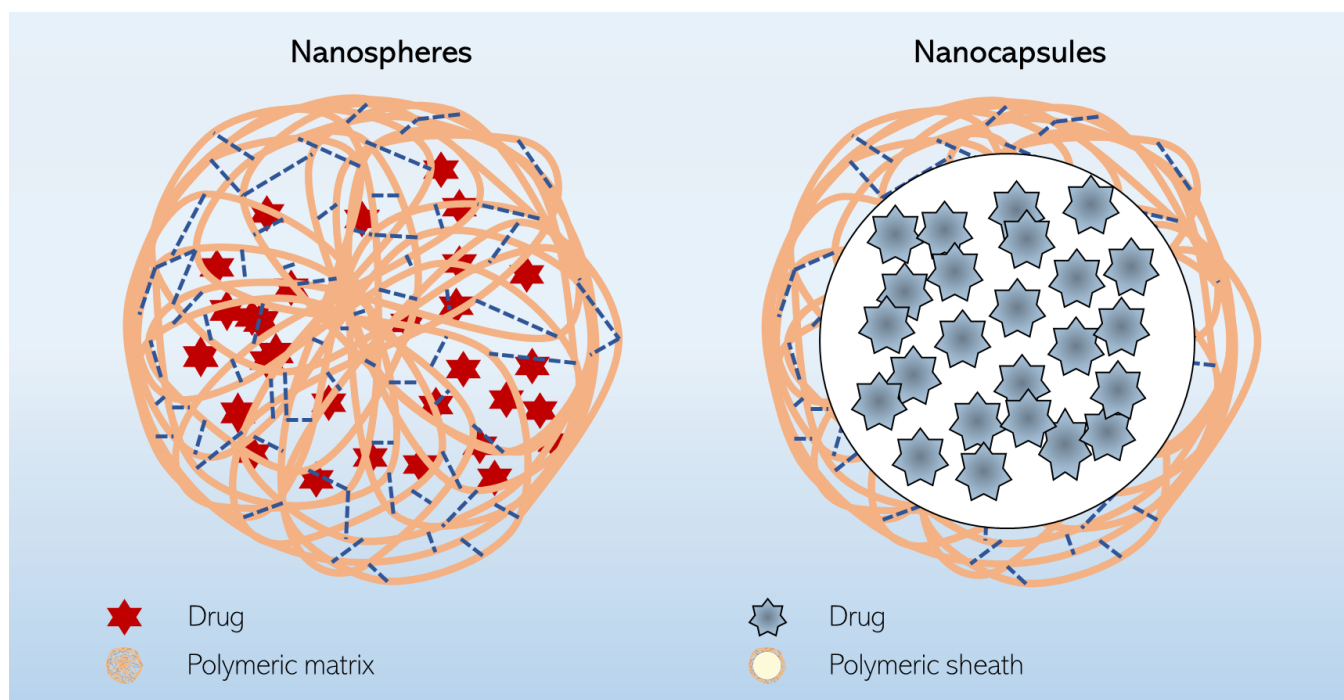


Figure 2. Representation of polymeric nanoparticles types according to drug encapsulation: Nanospheres (left) and Nanocapsules (right).

There is a considerable amount of literature describing PNPs synthesis methods that highlight the easiness of obtaining nanoparticles with physicochemical (e.g., size, morphology, physical stability), drug delivery (e.g., controlled and targeted release), and biological (e.g., immunogenicity, biocompatibility) properties precisely engineered (42,46–48). In consequence, polymer-based NPs have been extensively explored for encapsulating a wide variety of therapeutic agents, including nucleic acids (e.g., pDNA, siRNA), proteins, and peptides, where highly efficient drug encapsulation results have been commonly reported (10,11). On the other hand, many *in vivo* investigations have revealed the ability of PNPs to overcome biological barriers (e.g., blood-brain barrier, cell membranes) while protecting drugs from fast systemic clearance or enzymatic degradation and enhancing biodistribution and bioavailability (45,49). Furthermore, researchers have reported that surface chemical modifications (e.g., antibody-, peptide-, aptamer-conjugations) of the polymer-based NPs can endow the NPs with an active tissue targeting apart of their intrinsic passive tissue targeting (46,50,51).

Structurally, PNPs can be formed from natural (e.g., chitosan, alginate, hyaluronic acid) or synthetic (e.g., polyethylene glycol, poloxamers, polyvinyl alcohol) polymers (45). Thus, a myriad of polymers have been proposed as drug nanocarriers (51). The most common examples include PLGA-, PLA-, chitosan-, PEG-, and PVA-based nanoparticles (49). However, the literature reflects the preference of using natural polymers in the design of drug delivery nanosystems as they are, usually, more biocompatible and biodegradable than the synthetic ones (52,53). Additionally, many observations have identified that the hydrophobic character of polymers is a determining factor in the opsonization of NPs by serum proteins (e.g., C3, C4, and C5), which triggers their rapid elimination from the blood circulation (23,45,54). As a result, polymer-based nanoparticles owning a hydrophilic surface have been described as ideal drug transporters (45,55,56).

5.3. Physicochemical and biological considerations for polymer-based nanoparticles used in drug delivery applications

The characterization of polymer-based nanoparticles is a pivotal stage in the development of nanoparticle-based formulations (nanoformulations) for medical applications (57). It aims at anticipating the *in vivo* pharmacological performance of NPs by identifying their physicochemical and biological properties through diverse analytic techniques (58). Thus, the characterization is a vast interdisciplinary field that involves different fields, including materials science, physics, medicine, chemistry, and biology (59). Outstandingly, various studies have correlated the size, size distribution, morphology, charge, and chemical composition of nanoparticles with the drug encapsulation efficiency, cellular uptake of nanoparticle, drug biodistribution, nanoparticle biocompatibility, and drug bioavailability (45,57). In this section, the main physicochemical and biological properties of nanoparticles, including their size, size distribution, morphology, chemical composition, surface

characteristics, drug encapsulation, drug release kinetics, biodegradability, and toxicity as well as the characterization techniques used are reviewed.

5.3.1. Nanoparticle size, size distribution and morphology

The biological performance of nanoparticle-based formulations is greatly influenced by the size, size distribution, and morphology of NPs (60). First, nanoparticle size has been identified as a determining factor in the nanoparticle-based formulation pharmacokinetics as it determines their clearance from the systemic circulation (34,61). Numerous observations have described that NPs smaller than 5 nm are prone to suffer renal clearance, nanoparticles larger than 10 nm are cleared by the RES system, and particles larger than 150 nm may be gathered in the lungs, spleen, and liver (62). Additionally, nanoparticles ranging from 50 nm to 300 nm are capable of avoiding renal clearance as well as being distributed along tumor interstitium (42,45). In contrast, nanoparticles ranging about 10 nm to 200 nm tend to passively target tumor tissues due to the enhanced permeability and retention (EPR) effect (63). Hence, these characteristics must be considered in order to engineer an efficient drug delivery nanosystem according to the therapeutic application.

Particle size distribution refers to the heterogeneity degree of a nanoparticle population (64). Generally, the particle size distribution is expressed by a dimensionless index, the so-called polydispersity index (PDI) (59). This index can be understood either as the ratio of the weighted average molecular weight (M_w) and the number average molecular weight (M_n) (65) or as a result of calculations defined in the standard document ISO 22412:2017 (66). The first definition belongs to the estimation of PDI through chromatographic techniques (e.g., size exclusion chromatography) (59,66). In contrast, the second one corresponds to the use of spectroscopic techniques (e.g., dynamic light scattering) (67). Even though the first PDI definition is useful in the field of polymer science (66), this work will employ the second one in all subsequent sections. In this sense, the polydispersity index numerically ranges from 0 to 1, where values lower than 0.05 correspond to monodisperse nanoparticle populations, and values greater than 0.7 depict widely polydisperse nanoparticle populations (67). Since the pharmacological performance of nanoparticle-based formulations is mainly governed by the particle size, the PDI of nanoparticles has to be controlled to obtain nanoparticle populations as much homogenous as possible (59). Therefore, in the case of PNPs for drug delivery applications, a PDI value close to 0.2 is commonly considered adequate as it shows a low polydisperse population of NPs (66,68).

On the other hand, the morphology of nanoparticles plays a crucial role in several critical aspects directly related to the pharmacological performance of therapeutic nanoformulations, such as solubility, biodistribution, half-life in blood circulation, toxicity, and cellular uptake (11,45). Usually, PNPs are found as spherical morphology nanoparticles, although other morphologies (e.g., cylindrical)

have also been described (57). Among the different morphologies, spherical polymer-based NPs have been identified as the nanoparticles with better capacity to elicit their cellular uptake (11).

The recommended techniques for the characterization of the nanoparticle's size, size distribution, and morphology include Dynamic Light Scattering (DLS) and Electron Microscopy (e.g., Transmission Electron Microscopy (TEM), Scanning Electron Microscopy (SEM)) (33,45,69). On the one hand, DLS is a spectroscopic technique used for the indirect characterization of nanoparticle size and PDI of spherical nanoparticles in Brownian motion (70). Here, the calculus of the hydrodynamic size of nanoparticles, defined as the size of a solvated solid sphere particle, is used as an approximation to the actual nanoparticle size (67). On the other hand, electron microscopy enables the direct evaluation of nanoparticle size, size distribution, and morphology through the incidence of electron beams to a sample of NPs (71). Noteworthy, in the case of particles structured by low electron density materials, such as natural polymers, liposomes, or proteins, the dyeing with heavy metal stainings (e.g., phosphotungstic acid or uranyl acetate) is required in order to visualize the NPs (45).

5.3.2. Nanoparticle composition

Similar to nanoparticle size, size distribution, and morphology, the composition of NPs influences their pharmacological performance, especially the toxicity, immunogenicity, diffusion through biological barriers, cellular uptake, and systemic clearance (59). Biodegradable, non-antigenic, non-bioaccumulating, and non-toxic polymers are ideal for assembling drug delivery nanosystems (9). In this regard, the polymers included in the FDA's GRAS materials list are usually chosen (72). Thus, the characterization of the nanoparticle composition is essential in the design of nanoformulations since it enables to elucidate the elemental composition of nanoparticles (73). As a consequence, it analytically reveals if nanoparticles are correctly composed of the desired constituents (74). To this end, spectroscopic techniques, such as infrared spectroscopy, fluorescence spectroscopy, and nuclear magnetic resonance, are habitually used (75–77).

5.3.3. Nanoparticle surface charge

It is widely recognized that the nanoparticle surface charge is a valuable characteristic to determine the pharmacokinetics of nanoparticle-based formulations (78). Indeed, a vast amount of literature states that positively charged nanoparticles can hold electrostatic interactions with cell membranes, which promotes their cellular uptake (79). In the case of drug delivery polymer-based nanosystems, it has been found that the presence of polyamines on the surface of NPs can remarkably improve the drug delivery intracellularly as their protonation in endosomal acidic environments elicits the well-described proton-sponge effect (59). Furthermore, it has been indicated that the nanoparticle surface charge impacts their physical stability while they are colloiddally suspended (80).

Nowadays, there is no satisfactory analytical technique for the direct characterization of the surface charge of nanoparticles (60). However, the evaluation of the surface charge can be performed indirectly by measuring the electrical potential of the slipping plane of nanoparticles dispersed in an aqueous medium (**Figure 3**), usually referred to as the zeta potential (ζ -potential) (81). The methods commonly used to characterize this potential include phase analysis light scattering (PALS), tunable resistive pulse sensing (TRPS), and electrophoretic light scattering (ELS) (59,60,81). Since ζ -potential is an indicator of surface charge of nanoparticles, it is widely used for the study of nanoparticle-based formulations stability (82). In this sense, nanoformulations with an absolute zeta potential higher than 30 mV are considered stable as NPs electrostatically repel each other with enough energy to prevent their aggregation and precipitation (81,83).

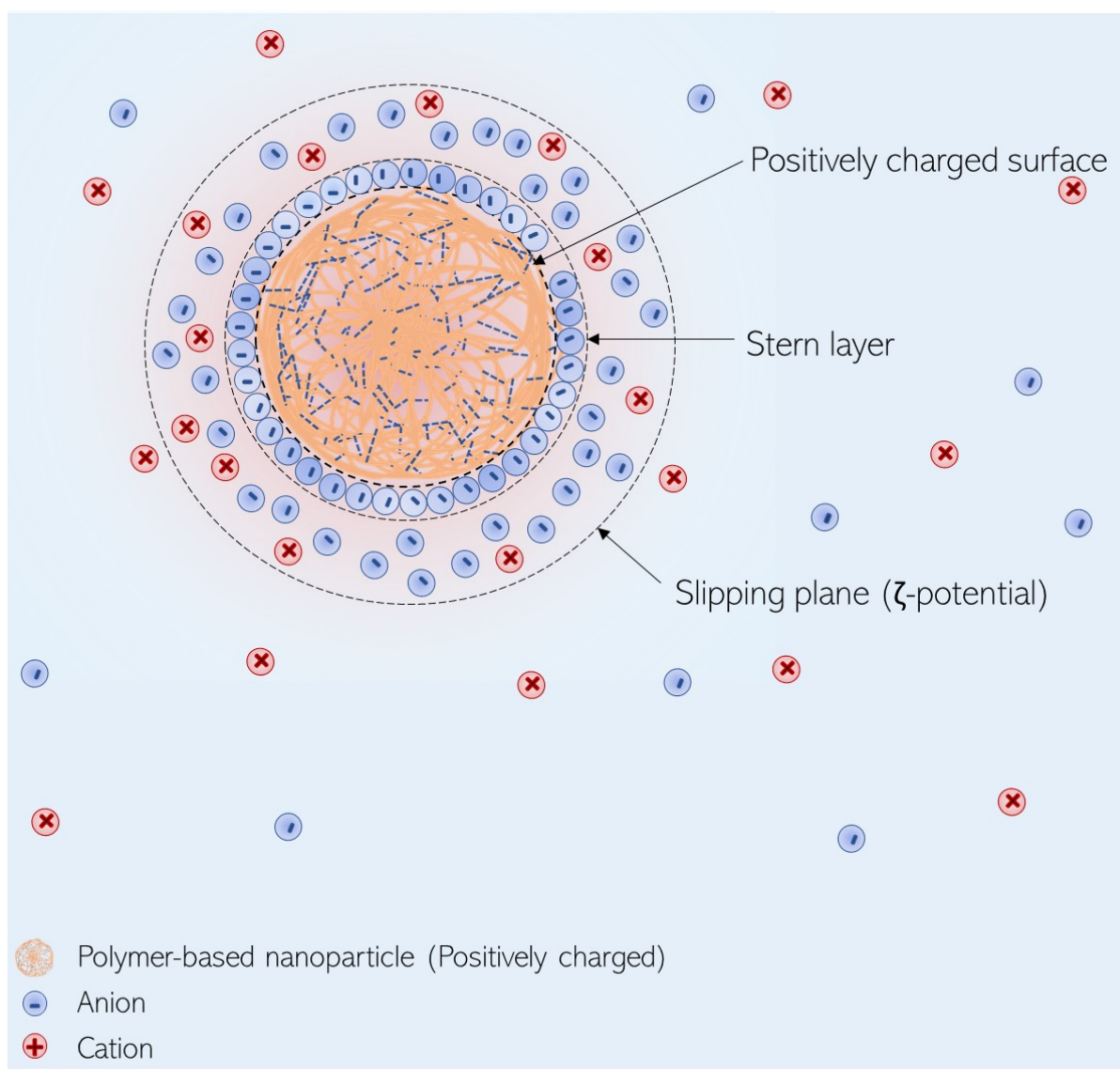


Figure 3. Diagram of electric potential layers of a polymer-based nanoparticle dispersed in an aqueous medium. The zeta potential refers electric potential measured in the slipping plane of the nanoparticle.

5.3.4. Drug loading and release

Profiles of both drug loading and drug release are the principal criterion in the quality evaluation of nanoparticle-based formulations (59). Depending on the drug encapsulation method, the therapeutic agent can be loaded into the PNPs by either covalent interactions, physical entrapment (non-covalent interactions), or surface adsorption (**Figure 4**) (84). The amount of loaded drug in a nanosystem can be determined by quantifying its drug encapsulation efficiency (EE%), namely, the percentage of the drug retained by the NPs relative to the total drug used for nanoencapsulation (85).

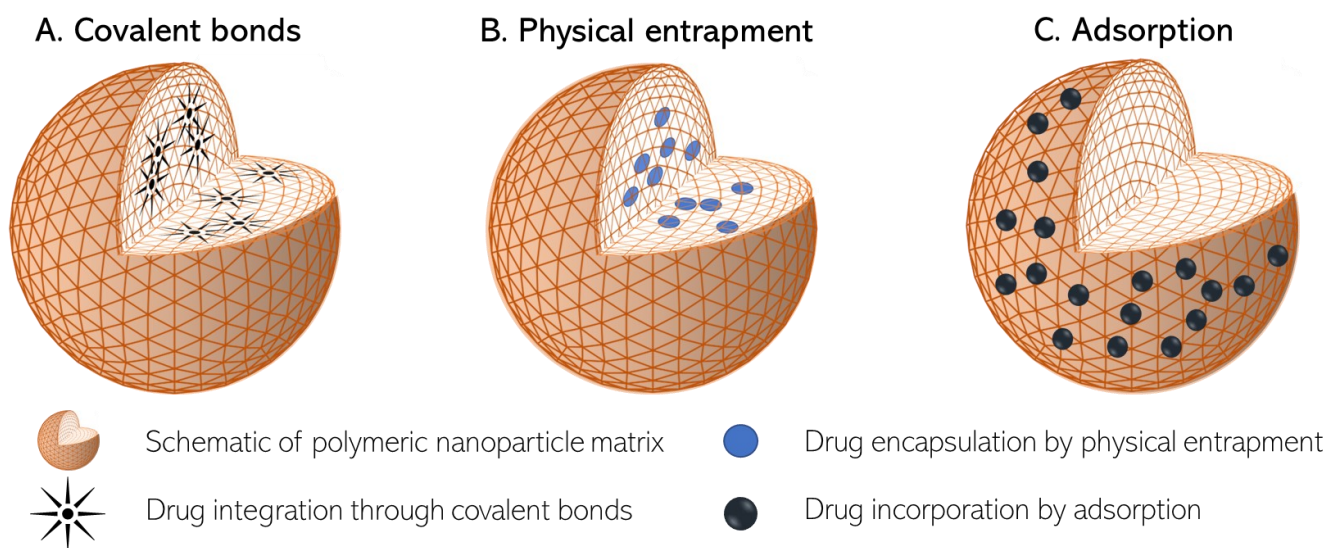


Figure 4. Methods of drug loading into polymer-based nanoparticles: (A) encapsulation by covalent interactions between polymer chains and drugs, (B) encapsulation by physical entrapment of drug into the polymeric matrix, and (C) drug encapsulation by drug adsorption onto the nanoparticle surface.

Drug release is understood as a stimulus-dependent process, where the encapsulated drugs are discharged from the NPs through drug diffusion, degradation of the polymeric matrix, or both (**Figure 5**) (86,87). As drug delivery systems, PNPs should be engineered to release the therapeutic agents in a controlled fashion in order to maintain the drug concentration inside its therapeutic window longer (59). At present, *in vitro* characterization of polymer-based NPs drug release kinetics has been performed via several methods, such as continuous flow (FC), sampling and separation (SS), and dialysis (DM) (88). In general, these studies aim at stressing the nanocarriers under simulated physiological conditions and, therefore, establish an *in vitro-in vivo* correlation (IVIVC) (89).

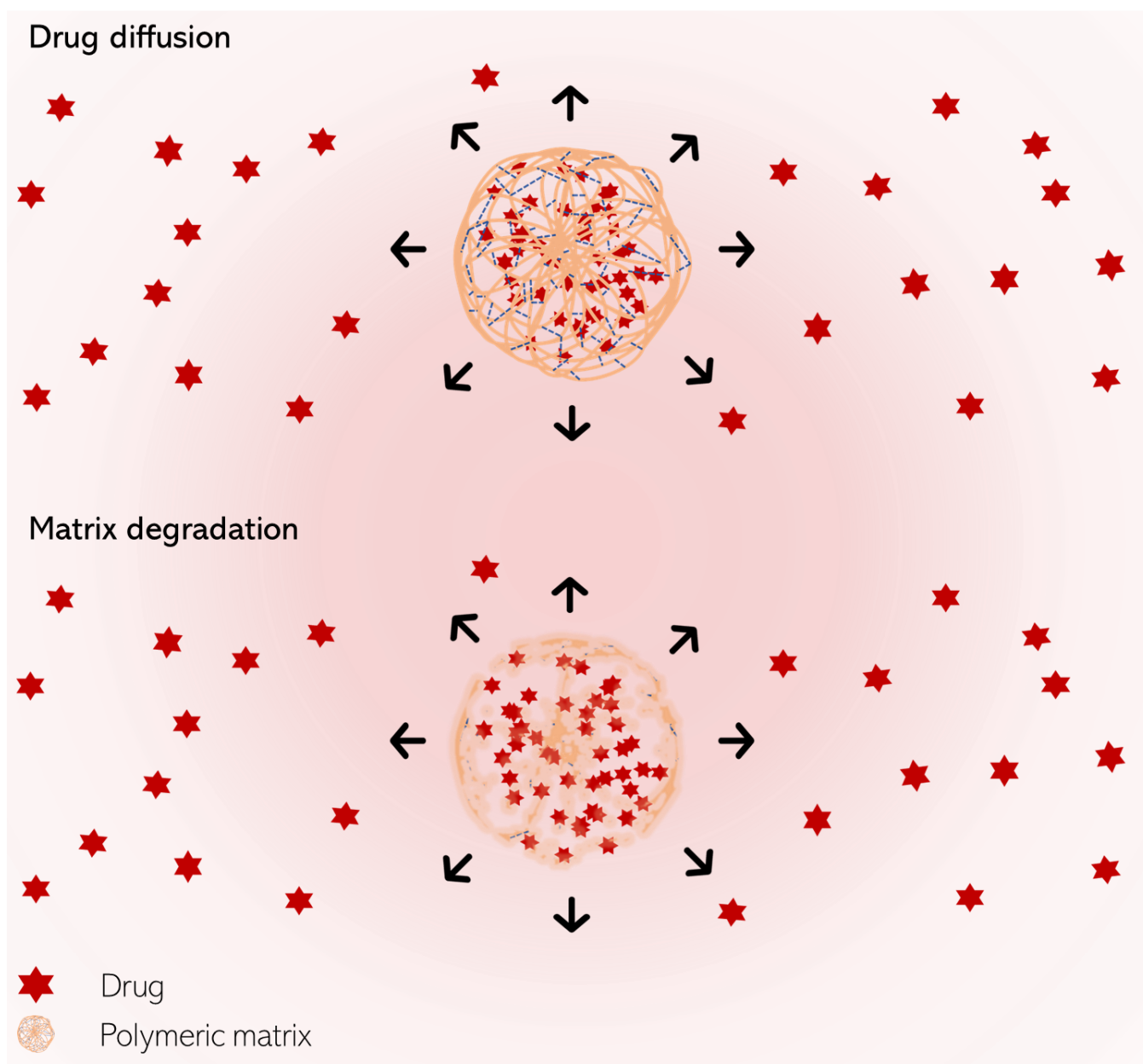


Figure 5. Illustration of drug release from the NPs. Drug diffusion (upper) and polymer matrix degradation (lower).

5.3.5. Polymer-based nanoparticles and cell viability

Drug safety is the essential criterion in drug development and, therefore, must be the principal aim in the design of therapeutic nanoformulations (59). While the use of non-toxic and biocompatible polymers is the first step toward the design of safe drug delivery nanosystems, it does not entirely imply the absence of cytotoxicity (9). Both physicochemical and biological properties of NPs, such as their reactivity and interactions with biosystems, have greater relevance in their toxicity (33). Moreover, nanoparticles may bear residual toxicity as traces of reagents used for their synthesis can remain in their structure (15). Thus, the cytotoxic behavior of NPs must be evaluated to determine their suitability for medical applications (59). To date, numerous cytotoxicity assays (e.g., dye exclusion, colorimetric,

fluorometric, and luminometric assay) have been well adapted to the evaluation of the *in vitro* toxicological profile of polymer-based nanoparticles (90). In this sense, the cytotoxicity assays based on the measurement of the *in vitro* metabolic activity of cells through colorimetric techniques, such as MTT (3-(4,5-dimethylthiazol-2-yl)-2,5-diphenyltetrazolium bromide) assay (MTT assay) or LDH (lactate dehydrogenase) assay (LDH assay), are the most used thanks to their simplicity, safety, high reproducibility, and high sensibility (91,92).

5.3.6. Cellular uptake

The design of drug delivery nanosystems that can be efficiently internalized by cells is one of the most significant challenges in current medicine (59,62). As is well known, the cellular membrane is a highly selective barrier aimed at protecting cells by limiting the intracellular traffic of foreign agents (42). However, numerous observations have associated the nanoparticles, especially polymer-based nanoparticles, with the capacity to be easily incorporated and degraded in cells (61). Possible mechanisms of NP cellular uptake are described to occur in a size-dependent manner, mainly via endocytic pathways (e.g., phagocytosis, macropinocytosis, and receptor-mediated endocytosis) (8,93). Several studies have reported that nanoparticles smaller than 200 and 500 nm might be internalized in cells through the clathrin-mediated and the caveolae-mediated endocytosis, respectively (42). However, the cellular uptake of NPs by phagocytosis and macropinocytosis has been observed and may happen in a non-selective way (45). Although nanoparticle size is imperative in NP cellular uptake, the nanoparticle morphology and surface charge are also significant (11), as mentioned in previous sections. Besides, cell-specific uptake properties might influence the efficiency of nanoparticle internalization (45,57). In this regard, the cellular uptake of nanoparticles can be evaluated *in vitro* through fluorimetric, radiometric, or confocal microscopic analysis of cells co-incubated with nanoparticles loaded with fluorescent or radiolabeled probes (65,94,95).

5.4. Chitosan nanoparticles as protein delivery systems

Chitosan (CS) is one of the most employed hydrophilic polymers in biomedical research owing to its pharmaceutical advantages, including high biocompatibility, non-antigenicity, and high biodegradability (96,97). Structurally, CS is a natural copolymer composed of β -(1-4)-linked D-glucosamine and N-acetyl-D-glucosamine monomers linearly and aleatory distributed (13,84,98). It was first described by Rouget in 1859 as a deacetylated variant of chitin (**Figure 6**), a natural and very abundant polymer (14,15). At present, it is categorized as a GRAS material by the FDA (12). Chitosan owns primary amine groups responsible for inducing most of its biological effects, such as mucoadhesiveness, antibacterial activity, fungicide activity, and hemocompatibility (15,99), besides conferring it a polycationic character (98,100). Depending on its source and method of obtaining, both its degree of deacetylation (DD) and molecular weight (MW) can vary in a range of 40% – 90% and 50

– 400 kDa, respectively (15,96,101). Therefore, various types of CS can be obtained. Low molecular weight (LMW) CS has been proven to have better biological performance regarding solubility, biocompatibility, bioactivity, and biodegradability, as compared with other variants (102).

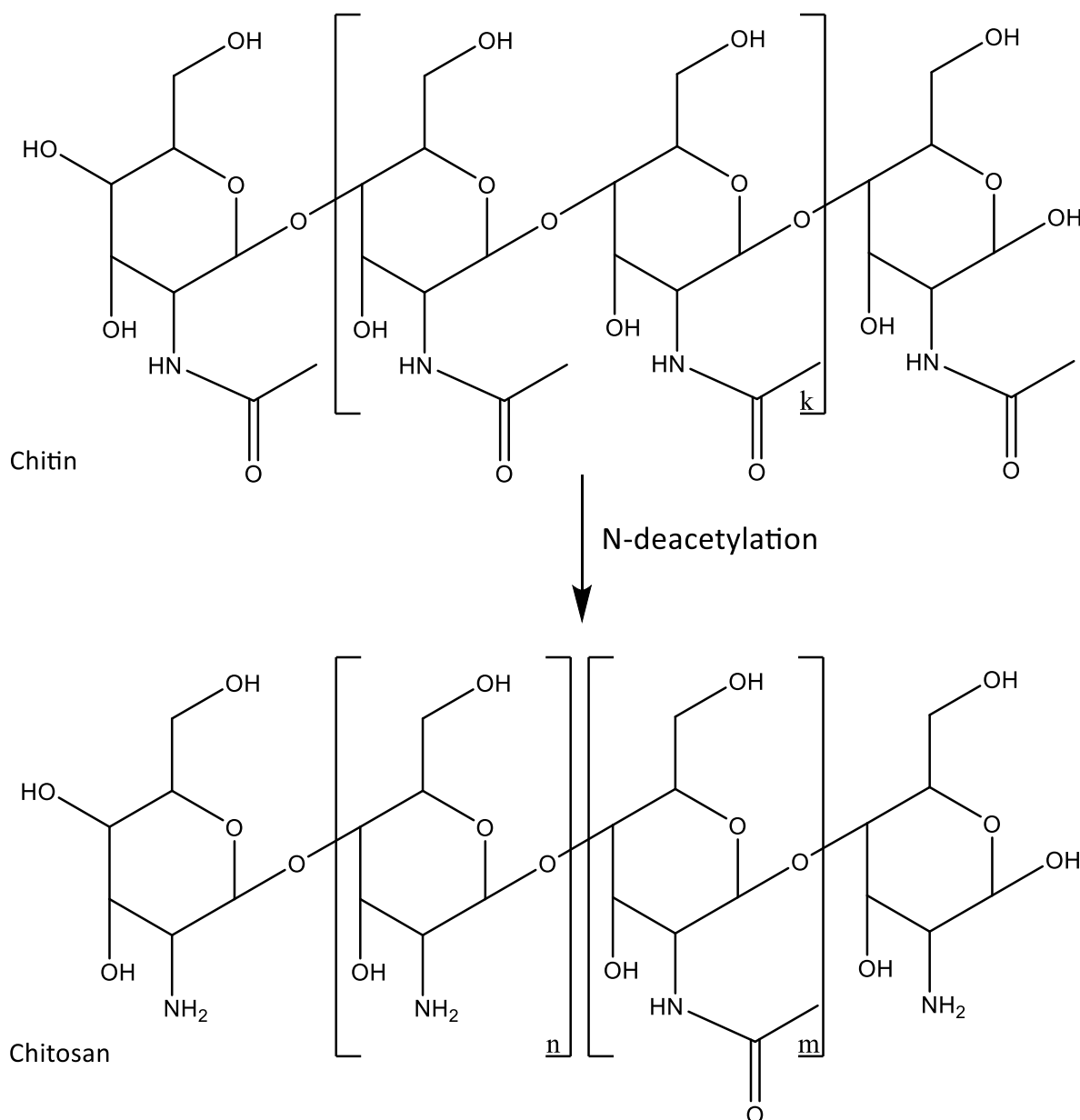


Figure 6. Schematics depicting the obtaining of chitosan from the N-deacetylation of chitin. DD is given by the ratio among N-acetyl-D-glucosamines (m) and D-glucosamines (n) present in the polymer. MW is determined by the length of polymer chains.

In the literature, the first investigations of CS as a biomaterial and pharmaceutical excipient dates back to the early 1990s (6). At that moment, chitosan applications were aimed to address tissue engineering, wound healing, and food packing (77,103). However, many studies have shown the suitability of CS to be used for drug delivery applications (104) since it bears *in situ* gelling and film-forming properties, which enable the controlled loading and release of drugs (94). Moreover, several *in*

in vivo investigations of CS-based drug delivery systems have reported on their high biodegradability as they can be easily degraded by some enzymes, including lysozyme and pepsin (13,105). In addition, CS-based drug delivery systems have also shown to trigger reversible reorganizations of the structural proteins Zonula Occludens-1 (ZO-1) and F-actin of epithelial cells, which elicits the opening of tight junctions (96). Consequently, CS-based drug delivery systems increase the paracellular permeability of epithelium and enhance the absorption of drugs (76).

Nowadays, the most widely studied chitosan-based drug delivery systems comprise hydrogels, films, tablets, microparticles, nanofibers, and nanoparticles (15). Among them, chitosan nanoparticles have been stated as ideal drug transporters since they enable improving the pharmacological performance of therapeutic formulations regarding several aspects, such as: controlled and sustained drug release, *in vivo* distribution, drug protection, and, therefore, therapeutic drug efficiency (13,94). Given the facts most of the therapeutic proteins are limited by formulation instability, proteolytic degradation, rapid clearance, immunogenicity, low solubility, low intracellular permeability, and reduced bioavailability, CS NPs have been extensively proposed as protein nanocarriers to optimize the therapeutic outcomes of protein formulations (84,105).

As protein delivery systems, CS NPs have shown to protect proteins from enzymatic degradation as well as to conserve their biological activity (96). Most of the research about the design of protein-loaded CS NPs has described the use of BSA as a model protein for encapsulation because of its economic advantages and the simplicity of its titration by colorimetric or imaging assays (84). In these studies, it has been shown that proteins can be encapsulated regardless of their hydrophobic character (103); however, the EE% can be strongly influenced by the encapsulation method (84). Besides, it has been widely proved that high DD chitosan is favorable to encapsulate greater amounts of protein owing to the formation of more electrostatic interactions among the proteins and the polymeric chains (84,100). Regarding the protein release behavior of protein-loaded CS NPs, several observations have described that, similarly to EE%, protein release is affected by the encapsulation method (84,106), proteins adsorbed on the surface of CS NPs being released faster than proteins entrapped in the polymeric matrix (12).

5.4.1. Chitosan nanoparticles by ionotropic gelation

There are numerous methods reported for the synthesis of protein-loaded chitosan nanoparticles, such as electrospraying, emulsion solvent diffusion, coacervation/precipitation, and ionotropic gelation (14). Among these methods, ionotropic gelation stands out as one of the most intensely employed method in the design of chitosan-based protein delivery nanosystems (107). This technique was first described by Calvo *et al.* in 1997 (14,108) as a simple and protein-friendly method aimed at synthesizing hydrophilic protein delivery nanosystems. Currently, ionotropic gelation is considered one of the easiest ways to manufacture chitosan nanoparticles in mild conditions with a low

polydispersity index (84,102). Physiochemically, it is based on the formation of nanoparticles through electrostatic complexation between chitosan polycationic chains and low molecular weight polyanionic species, such as sodium tripolyphosphate (TPP), cyclodextrin (CD), sodium sulfate, or dextran sulfate (DS) (96,109). To perform the process, chitosan is first dissolved in a slightly acidic aqueous solution (pH ~ 4.5) to protonate its primary amine groups, then, an aqueous solution of a polyanionic crosslinker, commonly TPP, is added dropwise at room temperature (RT) (99,110). As a result of the ionic crosslinking of the oppositely charged reagents, chitosan nanoparticles form spontaneously (**Figure 7**) (80). Since the synthesis of CS NPs by ionotropic gelation does not implicate the use of surfactants, organic solvents, or high temperatures, this process is appropriate for the encapsulation of proteins, which can be integrated to the nanoparticles by surface physisorption or non-covalent cross-linking (**Figure 8**) (108).

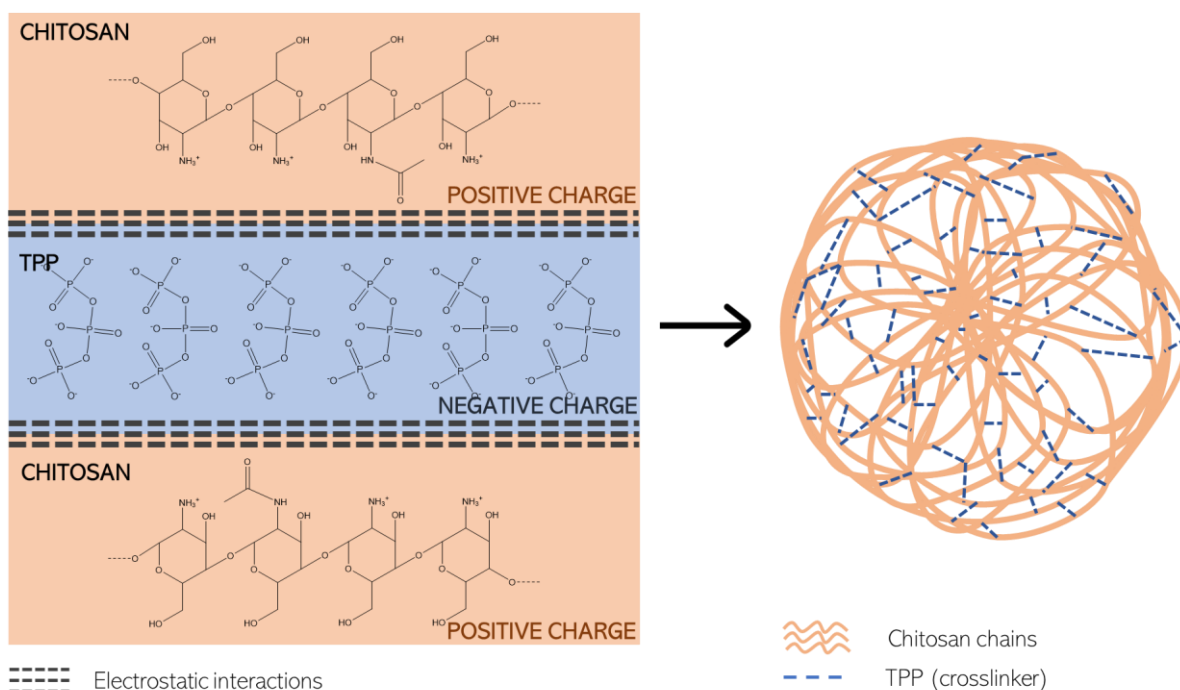


Figure 7. Proposed schematic drawing of CS NPs formation by ionotropic gelation.

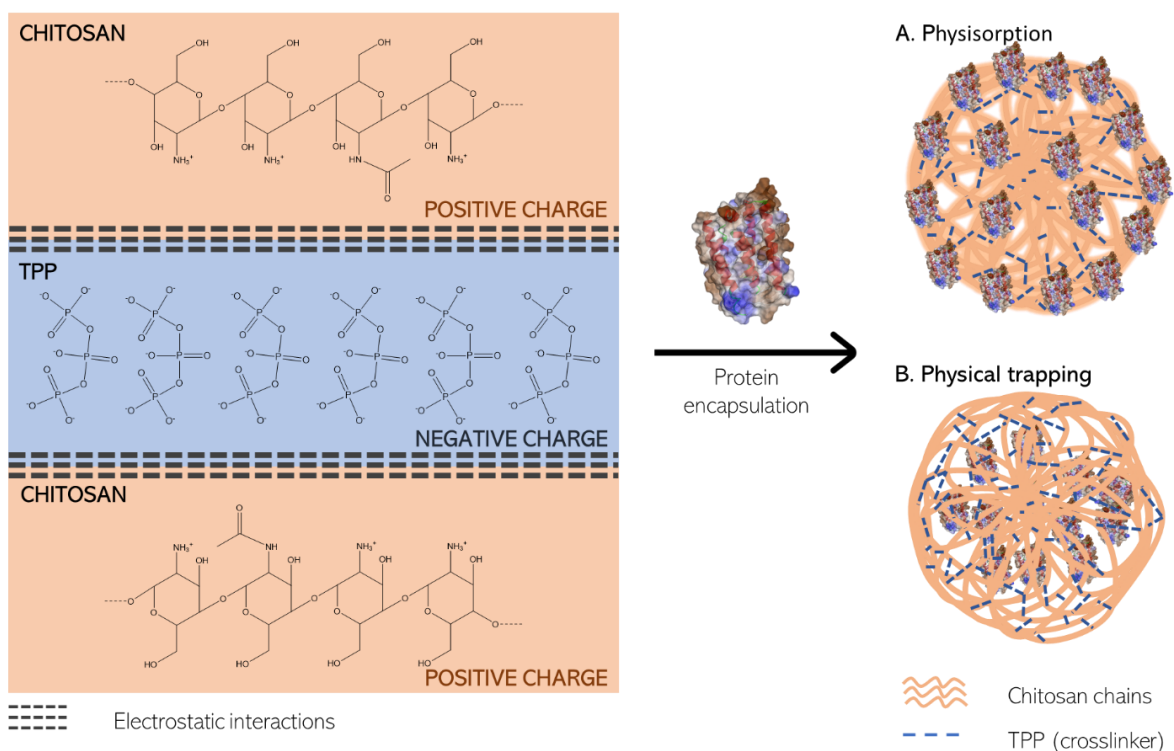


Figure 8. Schematic illustration of protein encapsulation in CS NPs by ionotropic gelation. If the protein is added to a dispersion of CS NPs already formed, **(A)** the protein is incorporated by physisorption to the NP surface. Otherwise, if the protein is prior homogenized with the CS solution or the TPP solution, **(B)** the protein is entrapped within the CS matrix by non-covalent crosslinking.

5.5. Porcine IFN α therapeutics

Interferon α is a small (19 kDa) pleiotropic immunomodulatory cytokine with antiviral and antiproliferative properties, present in all mammalian species (111). Structurally, this protein is arranged as a three-dimensional structure mainly composed of α -helical regions (**Figure 9**) (16). The biological activity of IFN α is attributed to the specific binding of its α -helical domains with particular cell surface receptors (111,112). As a response, antiviral-, antiproliferative-, or immunomodulatory-, cytoplasm signaling pathways are activated and, thus, the expression of several IFN-inducible genes is triggered (e.g., 2'-5'- oligoadenylate synthetase 1 (OAS1) and radical S-adenosyl methionine domain containing 2 (RSAD2)) (25,112). As an antiproliferative effector, IFN α has been found to activate apoptotic or antiproliferative mediator systems, such as 2-5A synthetase–RNase L and PKR–eIF2 (16). In the case of the IFN α -induced antiviral effect, the action mechanism has been widely described to be based on the endonuclease- or kinase-mediated deactivation of the replication of some viruses, such as Mengovirus and vesicular stomatitis virus (VSV) (112). On the other hand, the immunomodulatory activity of IFN α is induced via the up-regulated expression of cell surface markers (e.g., Fc receptors and b2-microglobulin) and cellular adhesion molecules, including intercellular adhesion molecule-1

(ICAM-1) (19). Worth mentioning, IFN α shows a cross-species activity *in vitro*; however, it possesses a species-specific activity *in vivo*, principally restricted by its glycosylation pattern (113).

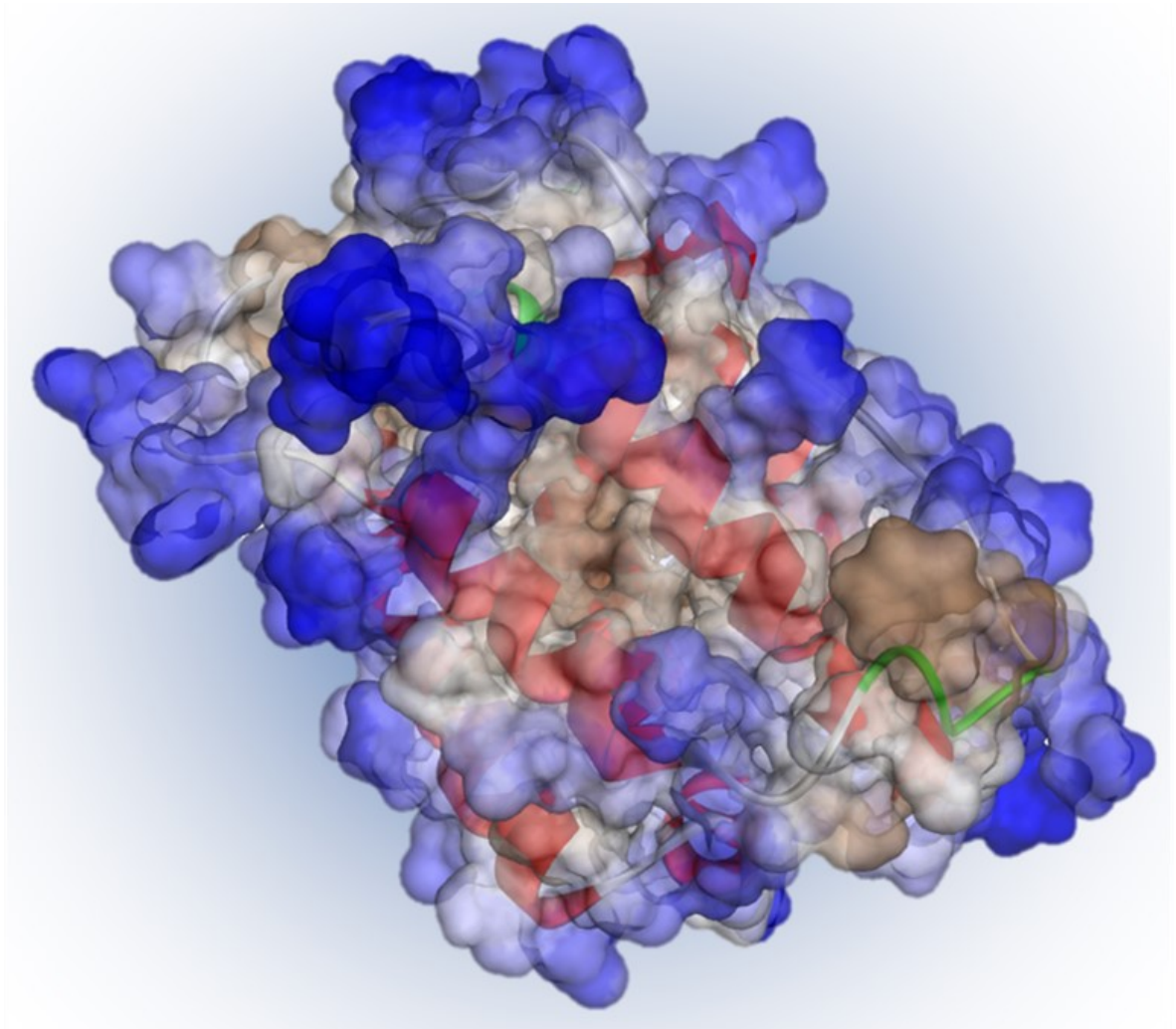


Figure 9. Molecular structure (ribbon and surface diagram) of IFN α . The hydrophobic character of the protein domains is shown from brown (more hydrophobic) to blue (less hydrophobic).

Owing to such essential biological activities, IFN α therapeutics exhibit an outstanding relevance in both human and veterinary medicine (24). To date, it has been used for the treatment of various diseases, including viral infections and numerous types of cancer (e.g., hairy cell leukemia, AIDS-related Kaposi's sarcoma, follicular non-Hodgkin's, lymphoma, or renal cell carcinoma) (25). In particular, several studies have identified porcine interferon α as a potent immunoadjuvant and antiviral therapeutic applicable in the prophylaxis and treatment of porcine infectious diseases, such as porcine reproductive and respiratory syndrome (PRRS), swine influenza virus infection, and porcine epidemic diarrhea (PED) (19,20,22). Accordingly, pIFN α formulations are appointed as an economically important tool with high incidence on the development of the global food industry (21). Similarly to most of the therapeutic proteins, the pharmacological efficiency of pIFN α is, however, quite limited by

its small molecular size, degradation, and rapid clearance from the systemic circulation by the reticuloendothelial system (23,26).

Nowadays, gold-standard strategies to extend the pIFN α half-life are principally focused on protein modifications (e.g., PEGylation, albumin binding, and immunoglobulin binding) (26). Nevertheless, modified forms of pIFN α are commonly associated with reduced biological activity and significant adverse effects (13). Therefore, the development of pIFN α nanoformulations has appeared as a promising solution (23,114). Although a vast amount of literature has described the design of nanoparticle-based IFN α formulations, the development of a suitable pIFN α nanoformulation remains an unexplored field (40).

Chapter IV

6. Materials and Methods

6.1. Materials

Low molecular weight (MW: 50-190 KDa) 75-85% deacetylated chitosan, sodium tripolyphosphate, bovine serum albumin, acetic acid, fluorescein isothiocyanate (FITC) and all the reagents used for molecular biology, cell culture, and immunological procedures, were purchased from Sigma-Aldrich (USA). Nitrocellulose membranes of 0.45 μm were acquired from Merck (Germany), and recombinant human interferon α -2b (Heberon Alfa R[®]) was obtained from Heber Biotec (Cuba). Recombinant porcine interferon α (rpIFN α) was kindly provided by the Pathophysiology Laboratory of the University of Concepcion (Chile).

6.2. Methods

6.2.1. Conjugation of Bovine Serum Albumin with Fluorescein Isothiocyanate

Bovine Serum Albumin was labeled with FITC following a slightly modified protocol proposed by Chaganti *et al.* (115). Briefly, BSA was dissolved (2 mg/mL) in 100 mM NaHCO₃ buffer pH 9 and mixed with FITC dissolved (1 mg/mL) in dimethyl sulfoxide (DMSO), at a ratio of 12.5:1 (BSA:FITC v/v). Next, the solution was gently stirred overnight in dark. Finally, the reaction mixture was dialyzed for 48 h in phosphate buffer saline (PBS) 1x to remove unreacted FITC from the solution using a 3.5 KDa cellulose dialysis membrane (Thermo Scientific, USA).

6.2.2. Synthesis of chitosan nanoparticles and protein-loaded chitosan nanoparticles

Chitosan nanoparticles (CS NPs) and protein-loaded chitosan nanoparticles (protein-loaded CS NPs) were synthesized by ionotropic gelation method as described by Canepa *et al.* (25) with some adjustments. First, CS was dissolved (2 mg/mL) in aqueous solution (pH 4.5 – 5) of acetic acid (1% - 2%) under magnetic stirring for 12 h, then filtered using a 0.45 μm nitrocellulose membrane. To load

the CS NPs with protein, specific amounts of protein were added to the filtered CS solution and homogenized by stirring for 30 min. In both cases, the nanoparticles were spontaneously formed by dropwise addition of TPP (2 mL, 1.5 mg/mL in water) to the CS solution using a KDS 200 syringe infusion pump (USA) with a 21G1 1/2 needle, at a flow of 15 mL/h, under magnetic stirring, and at RT. Finally, the nanoparticle suspensions were magnetically stirred (30 – 120 min) at RT and stored at 4 °C.

6.2.3. Nanoparticles characterization

6.2.3.1. Hydrodynamic diameter, polydispersity index, and zeta potential

Hydrodynamic diameter, polydispersity index, and zeta potential of CS NPs and rpIFN α -loaded CS NPs were characterized by Dynamic Light Scattering, using a Malvern Zetasizer Nano ZS90 (UK) equipped with a He-Ne 633 nm laser, using a method described by Du *et al.* (22). The nanoparticle batches were diluted 1:10 and 1:100 in water (v/v) and transferred to Malvern disposable polystyrene cuvettes DTS0012 and folded capillary zeta cells DTS1070, for size-related and zeta potential measurements, respectively. Results were acquired and analyzed using Malvern Zetasizer software version 7.01.

6.2.3.2. Morphology

The morphology of CS NPs and rpIFN α -loaded CS NPs was studied using Transmission Electron Microscopy (TEM, JEOL/JEM 1200 EX II, Japan), as described by Sreekumar *et al.* (107). The nanoparticle samples were diluted in water (1:100 v/v), cast on copper grids, and immersed in a uranyl acetate 4% solution for 30 s. Excess liquid was removed from grids using filter paper. Finally, grids were dried at RT before being observed in TEM.

6.2.3.3. Infrared spectroscopy

Attenuated Total Reflectance Fourier Transform Infrared Spectroscopy (ATR-FTIR) was used to characterize the chemical composition of CS NPs (PerkinElmer FTIR Spotlight 400 & Spectrum Frontier, USA), identically as described by Othman *et al.* (109). To this purpose, CS NPs were centrifuged (10000 rpm, 30 min) and the pellets were dispersed in PBS 1x. The nanoparticles were vacuum freeze-dried prior to infrared characterization. The Infrared spectra from the NPs were acquired and analyzed using the software Spectrum (10-03-06.0100) & SpectrumIMAGE (R1.7.1.0401).

6.2.3.4. Fluorescence spectroscopy

Fluorescence spectroscopy was used to confirm both the conjugation of BSA with FITC and the encapsulation of FITC-conjugated BSA ((FITC)BSA) into CS NPs (Multiphoton Laser Scanning Microscope Zeiss LSM 780 NLO, Germany), as previously proposed by Yeh *et al.* (116) with some modifications. To this end, the (FITC)BSA-loaded CS NPs were centrifuged (10000 rpm, 30 min) and the pellets were dispersed in PBS 1x. Finally, both, FITC-conjugated BSA solution and the (FITC)BSA-loaded CS NPs dispersed in PBS 1x were characterized. The fluorescence spectra from the (FITC)BSA solution and the (FITC)BSA-loaded CS NPs were obtained and analyzed using the software ZEN 2.3 SP1 (14.0.0.201).

6.2.3.5. Encapsulation efficiency of rpIFN α

The encapsulation efficiency from the rpIFN α -loaded CS NPs was determined using Size Exclusion High-Performance Liquid Chromatography (SEC-HPLC) by quantifying the amount of free rpIFN α in the supernatant of a NP synthesis mixture, as described by Xu *et al.* (50) with few modifications. Chromatographic separation was achieved using a TSKgel G2000SW size exclusion column (7.5 mm ID \times 60 cm \times 2; Tosoh Bioscience GmbH, Germany). For this, a positive reference consisting of a rpIFN α solution (8 mL, 30 μ g/mL in PBS 1x), and a negative reference (the supernatant of a centrifuged batch of CS NPs (10000 rpm, 30 min)) were used to measure the total amount of protein and the polymer interference, respectively. Next, the supernatant obtained from the centrifugation of a rpIFN α -loaded CS NPs batch was compared with the controls to establish the quantity of free rpIFN α . The EE% was calculated according to the following equation:

$$EE\% = \left[\frac{Rp - (Sx - Rn)}{Rp} \right] * 100\% ;$$

where Rp is the total amount of rpIFN α used for encapsulation, Rn is the result of the polymer interference (negative reference), and Sx is the amount of non-encapsulated rpIFN α .

6.2.3.6. *In vitro* protein release studies

The protein release kinetics from the rpIFN α -loaded CS NPs was characterized *in vitro* as indicated by Damiasi *et al.* (63). Briefly, CS NPs and rpIFN α -loaded CS NPs were synthesized and centrifuged (10000 rpm, 30 min). The pellets were dispersed in PBS 1x (pH 7.4) and aliquots of 2 mL were placed in a shaker at 150 rpm and 37 °C; to simulate physiological conditions. Every single sampling time, aliquots from each condition were withdrawn and centrifuged. Finally, the protein concentration of the supernatants was determined by using the Thermo Scientific™ Micro BCA™ Protein Assay Kit (USA) following the manufacturer's protocol (117).

6.2.4. Experiments with cancer cell lines

Porcine Kidney-15, PK-15 (ATCC CCL-33) and Human Epithelial type 2, HEp-2 (ATCC CCL-23) cell lines were maintained in Dulbecco's Modified Eagle Medium (DMEM) supplemented with penicillin (100 units/mL), streptomycin (100 µg/mL), and 10% (v/v) heat-inactivated fetal calf serum (FCS) at 5% CO₂ and 37 °C, as previously reported (25).

6.2.4.1. Cytotoxicity assay

The cytotoxicity of CS NPs and rpIFN α -loaded CS NPs was evaluated in PK-15 cells using the MTT (3-(4,5-dimethylthiazol-2-yl)-2,5-diphenyltetrazolium bromide) assay, as described by Jiang *et al.* (118) with some adaptations. First, the cells were treated with different quantities of both the CS NPs and the rpIFN α -loaded CS NPs (10, 50, 100, 500 µg) in 50 µL of DMEM supplemented with 1% of FCS. Non-treated cells in DMEM containing 1% of FCS and cells treated with Triton X-100 diluted in DMEM (0.1%) supplemented with 1% of FCS were set as viability and cytotoxicity controls, respectively. Subsequently, the cells were incubated at 37 °C and 5% CO₂. After 24 h, 50 µL of cell medium containing MTT (2 mg/mL) were added to each plate well. The incubation conditions were maintained for 4 h more to allow the reduction of MTT and, consequently, the formation of insoluble formazan crystals inside the cells. Next, unreacted MTT solution was removed by aspiration, and the crystals were dissolved by adding 100 µL of DMSO. Ultimately, the absorbance of each plate well was measured at 570 nm by the plate reader SPECTROstar Nano (BMG LABTECH, Germany).

6.2.4.2. Cellular uptake of (FITC)BSA-loaded CS NPs

Cellular uptake of (FITC)BSA-loaded CS NPs was visualized *in vitro* in HEp-2 cells, as reported by Chiang *et al.* (78) with some adjustments. The cells were seeded in a 24-well plate on sterile coverslips using DMEM containing 5% of FCS and incubated at 5% CO₂ and 37 °C. Once the cell monolayer confluence reached 60% – 80%, the cells were washed with fresh DMEM and co-incubated with 1 mL of DMEM containing (FITC)BSA-loaded CS NPs and 1% FCS at 5% CO₂ and 37 °C. For this, 4 mL of a just-prepared (FITC)BSA-loaded CS NPs batch synthesized with 240 µg of (FITC)BSA were centrifuged at 10000 rpm for 30 min, and the pellet was dispersed in 1 mL of culture medium. 24 h post-incubation, the cells were washed with DMEM. Then, the nuclei and mitochondria of the cells were stained by simultaneously adding Hoechst 33342 (Thermo Scientific, USA) at 0.1 µg/mL and MitoTracker® Red CMXRos (Thermo Scientific, USA) at 50 nM, respectively. Immediately, cells were incubated for 20 – 25 min at 37 °C in dark. Finally, non-retained dyes were removed from the cells by three washing steps using DMEM, following to the manufacturer's protocol (119,120). Finally, the cell

fluorescence images were obtained using an SP8 LIGHTNING confocal microscope (Leica Microsystems, Germany).

6.2.4.3. *In vitro* biological activity of the encapsulated rpIFN α

The biological activity of the encapsulated rpIFN α was determined *in vitro* by evaluating its capacity to induce antiviral activity against Mengovirus in HEp-2 cells, as indicated by Meager (112). For the assay, HEp-2 cells were seeded in 96-well plates at a density of 1×10^5 cells/mL with DMEM supplemented with 5% of FCS and incubated at 37 °C and 5% CO₂ for 24 h. Next, the culture medium was substituted by DMEM supplemented with 1% of FCS. Immediately, the cells were treated with commercial Heberon Alfa R® (1200, 600, 120, 60, 12, 6 IU) or with supernatants from a new *in vitro* protein release study of CS NPs or rpIFN α -loaded CS NPs (synthesized with 240 μ g of rpIFN α). Non-treated cells were used as a viral control. Subsequently, the cells were incubated for 24 h in the same previously described incubation conditions. Afterward, the cells were infected with Mengovirus and were let in incubation (37 °C and 5% CO₂) until to observe 100% cytopathic effect in the viral control (16 to 20 h). Cells without any treatment and infection were considered as viability control. After incubation, the cells were fixed and stained with crystal violet. Finally, the absorbance of each plate well was measured at 590 nm using the plate reader SPECTROstar Nano (BMG LABTECH, Germany).

6.2.5. Statistics

Unless otherwise mentioned, the results for the quantitative tests were obtained by averaging the measurements of at least three independent replicates. The results are expressed as mean \pm standard deviation (SD). Data were statistically analyzed employing the Student's t-test and the one-way analysis of variance (ANOVA), as appropriate, using RStudio software (version 1.1.456, USA). A p-value of $p < 0.05$ was considered statistically significant.

Chapter V

7. Results and Discussion

7.1. Synthesis of chitosan nanoparticles

7.1.1. Standardization of chitosan nanoparticles synthesis

Several chitosan nanoparticle synthesis variants based on ionotropic gelation were studied, aiming at synthesizing competent nanosystems for drug delivery applications. Hence, as depicted in **Table 1**, the concentration of acetic acid, the stirring rate of the CS-TPP solution, and the stirring time of the CS-TPP solution were systematically fine-tuned until obtaining CS NPs with optimal characteristics regarding size and size distribution, as discussed in the literature review.

The nanoparticles produced via each procedure were characterized using dynamic light scattering to assess their hydrodynamic diameter and their polydispersity index (**Table 2**). As a result, it was observed that CS NPs were obtained with a size range ~200 nm in all formulations. However, the PDI results broadly varied from 0.221 to 0.435, being the synthesis formulation std5, the one with the lowest PDI result (0.221) and, thus, allowing the synthesis of the most homogeneous NPs populations (66). Even though no statistical analysis could be conducted (n=1), this study suggests a possible correlation between the analyzed formulation parameters and size, and size distribution of synthesized NPs, which is consistent with previously reported results (107). Finally, based on these results, the synthesis formulation std5 was selected for further studies.

Table 1. Preparative parameters used in the standardization of chitosan nanoparticle synthesis.

Formulation code	Chitosan concentration (mg/mL)	Acetic acid concentration (%)	Acetic acid solution pH	Stirring rate of the CS solution (rpm)	TPP concentration (mg/mL)	CS:TPP ratio (v/v)	TPP solution addition flow (mL/h)	Stirring rate of the CS-TPP solution (rpm)	Stirring time of the CS-TPP solution (min)	Final Volume (mL)
std1	2	1	4.5 - 5	400	1.5	3:1	15	700	120	8
std2	2	2	4.5 - 5	400	1.5	3:1	15	700	120	8
std3	2	2	4.5 - 5	400	1.5	3:1	15	700	60	8
std4	2	2	4.5 - 5	400	1.5	3:1	15	700	30	8
std5	2	2	4.5 - 5	400	1.5	3:1	15	600	30	8

Table 2. Standardization results regarding the hydrodynamic diameter and PDI of nanoparticles (n=1).

Results		
Formulation code	Hydrodynamic diameter (nm)	PDI
std1	197.6	0.435
std2	195.8	0.392
std3	211.3	0.257
std4	209.0	0.253
std5	205.1	0.221

7.1.2. Reproducibility of the chitosan nanoparticle synthesis reaction

Several independent batches of CS NP synthesized employing the formulation std 5 were characterized by DLS in order to evaluate their reproducibility (**Figure 10**). As a result, the average hydrodynamic diameter and the average PDI of CS NPs were equal to 202.24 ± 6.24 nm and 0.24 ± 0.03 , respectively. Statistical analysis found no significant difference between the results of each CS NPs batch. This finding demonstrated that CS NPs can be synthesized from the ionotropic gelation-based formulation std5 reproducibly. Similar results were reported by Piras *et al.* (121) who reported ionotropic gelation reproducibility under their specific synthesis conditions. Finally, the formulation std5 was set as the default formulation for the synthesis of CS NPs in all the following analyses owing to such suitable results.

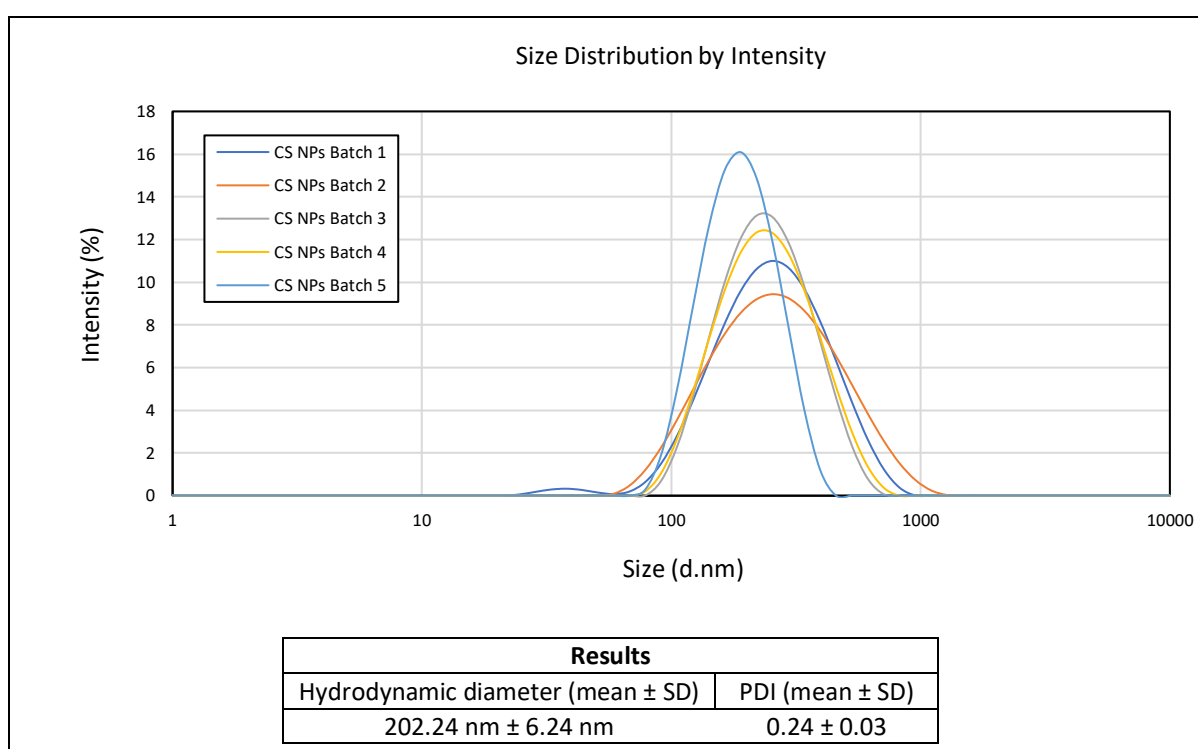


Figure 10. DLS characterization (size distribution by intensity) of chitosan nanoparticles synthesized using the formulation std5. Results are expressed as mean \pm SD (n=5).

7.1.3. Physical stability characterization

ζ -potential characterization was used to anticipate the physical stability of CS NPs in colloidal suspension, as seen in **Figure 11**. In response to this study, CS NPs showed a narrow ζ -potential distribution centered at +35.5 mV. First, the stability of colloiddally dispersed nanoparticles is directly correlated to the magnitude of their ζ -potential, NPs with values higher than 30 being widely considered as ideal (83). This said, this observation identified CS NPs as electrostatically stable systems in aqueous media, as indicated by He *et al.* (61). Besides, the positive ζ -potential, given by the presence of cationic CS chains in the surface of NPs (121), suggested that CS NPs may hold electrostatic interactions with

the negatively charged cell membranes (84). Accordingly, this result implied that CS NPs were prone to be transported and taken up by cells (122).

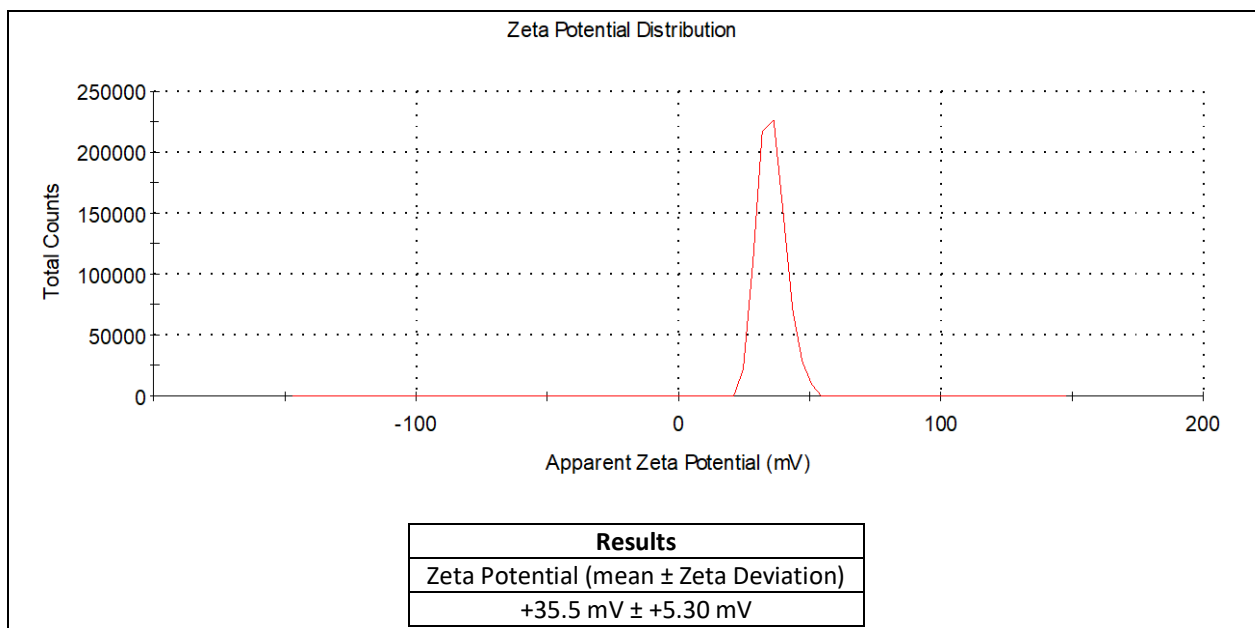


Figure 11. Zeta potential distribution of chitosan nanoparticles. Results are indicated as mean \pm Zeta Deviation.

7.1.4. Structural characterization

The structural characterization of the chitosan nanoparticles was performed through ATR-FTIR. Infrared spectra of several CS NPs samples are shown in **Figure 12**. As a result of the spectra analysis (**Table 3**), the nanoparticles were identified as being mainly constituted by CS, as reported by de Pinho Neves *et al.* (123). However, in addition to CS spectra, it was found the presence of signal bands belonging to phosphate groups of TPP at the wavenumbers 1260 cm^{-1} and 922 cm^{-1} , corresponding to P=O stretching and P-O-P stretching, respectively (69,74,124,125). Hence, consistent with Othman *et al.* (109), this finding corroborates the assembly of CS NPs mediated by electrostatic interactions between the ammonium cations of CS and the phosphoric anions of TPP.

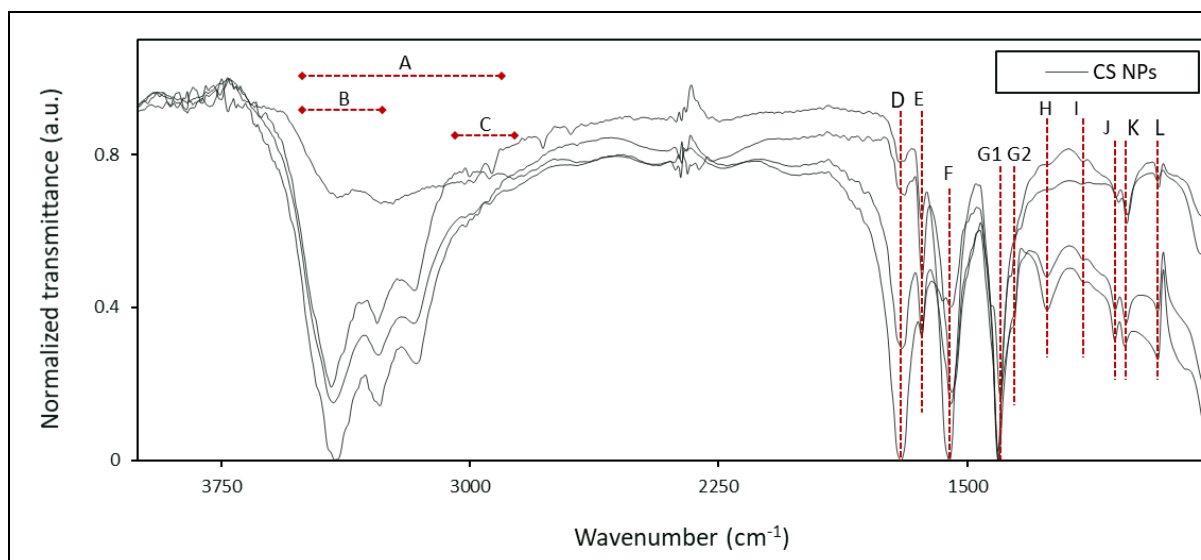


Figure 12. Normalized ATR-FTIR transmittance spectra of lyophilized chitosan nanoparticles.

Table 3. ATR-FTIR analysis of chitosan nanoparticles.

Peak	Wavenumber (cm ⁻¹)	Possible assignment	Ref
A	3500-2700	O-H stretching	(74,109,124–127)
B	3500-3300	N-H stretching, amine N-H stretching, amide	(74,125–127)
C	2900-2800	C-H stretching	(109,124)
D	1700	C=O stretching, carboxylic acid	(72,106,126–129)
E	1636	C=O stretching, amide	(79,106,109,129)
F	1550	N-H bending, amine C-N stretching, amide N-H bending, amide	(79,106,109,127–129)
G1 and G2	1408 and 1370	C-H bending	(79,125,129)
H	1260	P=O stretching	(69,74,124)
I	1144	C-N stretching, amine	(127,128)
J	1055	C-O-C stretching	(127,129)
K	1020	C-O stretching	(79,109,129)
L	922	P-O-P stretching	(69,125)

7.1.5. Morphology characterization

The morphology of CS NPs was examined by Transmission Electron Microscopy. As shown in **Figure 13**, TEM micrographs revealed the CS NPs as compact structured particles with spherical morphology. Hence, this result concurs with previous findings described in the literature (107,108,123,130). Besides, the actual sizes of CS NPs observed in TEM lend support to the nanoparticle hydrodynamic diameter measurements obtained by DLS.

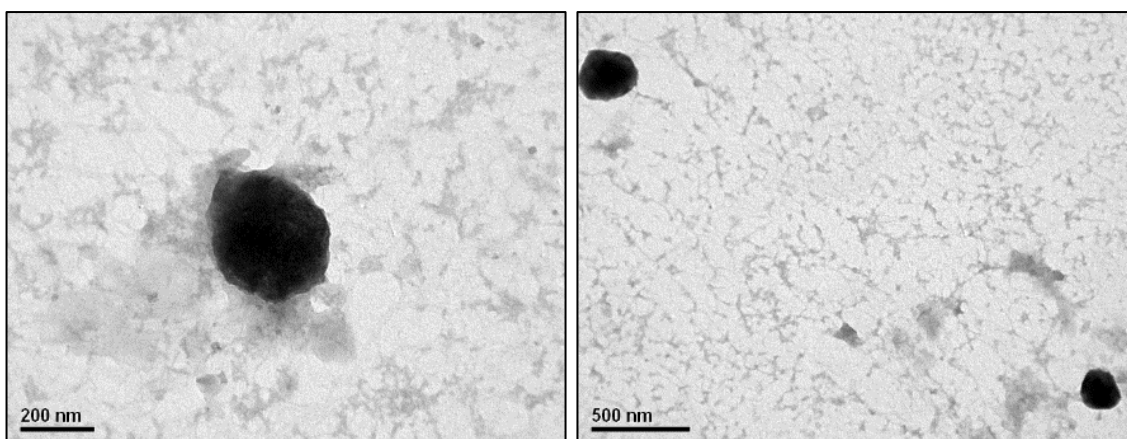


Figure 13. Transmission electron micrographs of chitosan nanoparticles.

7.1.6. Scaling of chitosan nanoparticle synthesis reaction

Batches of CS NPs were synthesized from volume-modified formulations in order to explore the effects of the total volume of reaction mixture on the size and size distribution of the nanoparticles. To this purpose, two new NPs synthesis formulations were designed by augmenting twice (16 mL) and five times (40 mL) the total volume of the reaction. The proportions between all reagents were conserved as in the default formulation. Finally, the results of each formulation were characterized by DLS and statistically compared with the results from the default formulation. The results are shown in **Figure 14**.

In the case of the 16-mL synthesis formulation, the statistical analysis found a significant ($p < 0.05$) difference in the CS NPs hydrodynamic diameter (212 nm); however, no variation was identified in the PDI result. Thus, it was shown that the population of CS NPs obtained via the 16-mL synthesis formulation was low polydispersity with an average size larger than the default CS NPs. Although increased, the hydrodynamic diameter of these CS NPs remained optimal for drug delivery applications (45). On the other hand, no significant difference was observed between the 40-mL CS NPs synthesis formulation and the default formulation regarding hydrodynamic diameter and PDI. Importantly, this study highlights the feasibility of eventually scaling up the synthesis of CS NPs with drug-delivery-suitable hydrodynamic diameter and PDI values (25).

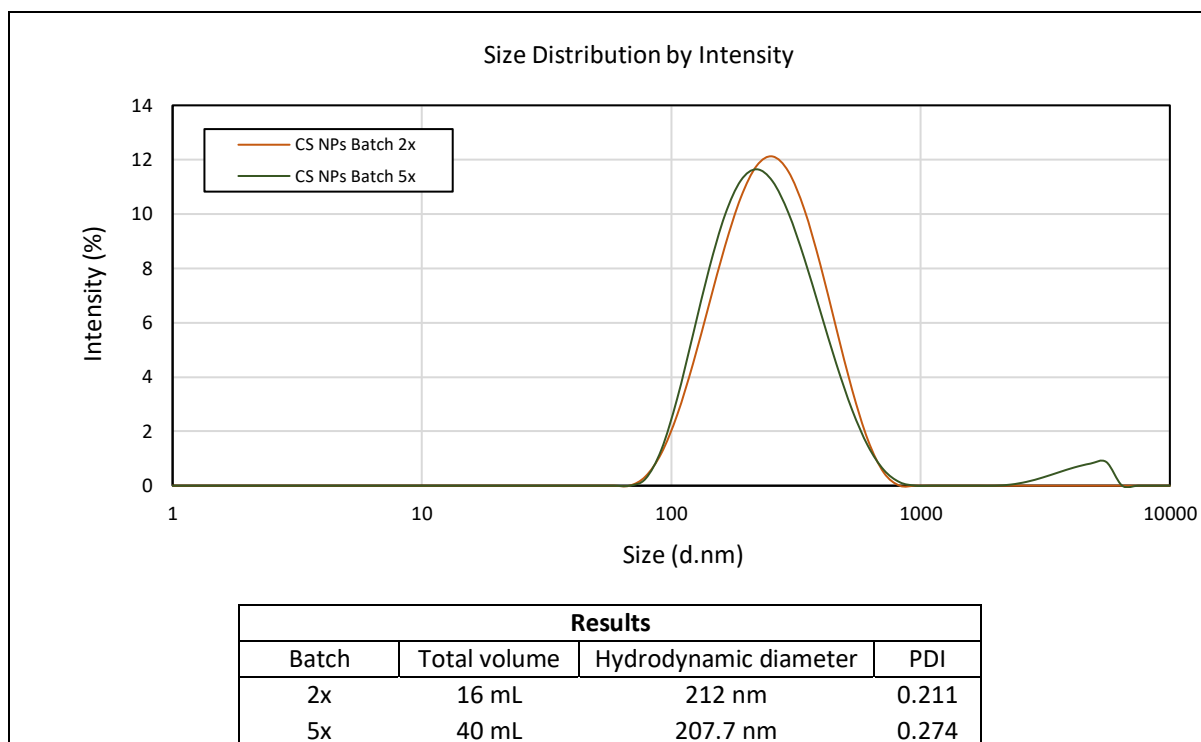


Figure 14. DLS characterization (size distribution by intensity) of CS NPs synthesized by volume-modified formulations (16 mL and 40 mL).

7.2. Synthesis of protein-loaded chitosan nanoparticles

7.2.1. Protein encapsulation

The ability of CS NPs to encapsulate proteins was firstly examined using (FITC)BSA as a model protein (63,78,116,131). In this regard, the default formulation for CS NPs synthesis was modified by mixing 24 μg of (FITC)BSA with the CS solution, preceding the addition of the TPP solution. Next, the fluorescent emission spectra from both (FITC)BSA solution and (FITC)BSA-loaded CS NPs were characterized using fluorescence spectroscopy. As presented in **Figure 15**, the resulting fluorescent emission spectra of the (FITC)BSA solution (**Figure 15 (A)**) and the (FITC)BSA-loaded CS NPs (**Figure 15 (B)**) revealed a maximum emission wavelength at 522 nm and 520 nm, respectively. As reported by Hermanson (132), the maximum emission wavelength of FITC is at about 520 nm. Accordingly, these results evidenced that, in the case of the (FITC)BSA solution, FITC was effectively conjugated to BSA and, to the case of the (FITC)BSA-loaded CS NPs, (FITC)BSA was successfully integrated into CS NPs. Finally, in complete agreement with Calvo *et al.* (108), these findings confirmed the viability of CS NPs to be used as protein delivery nanosystems.

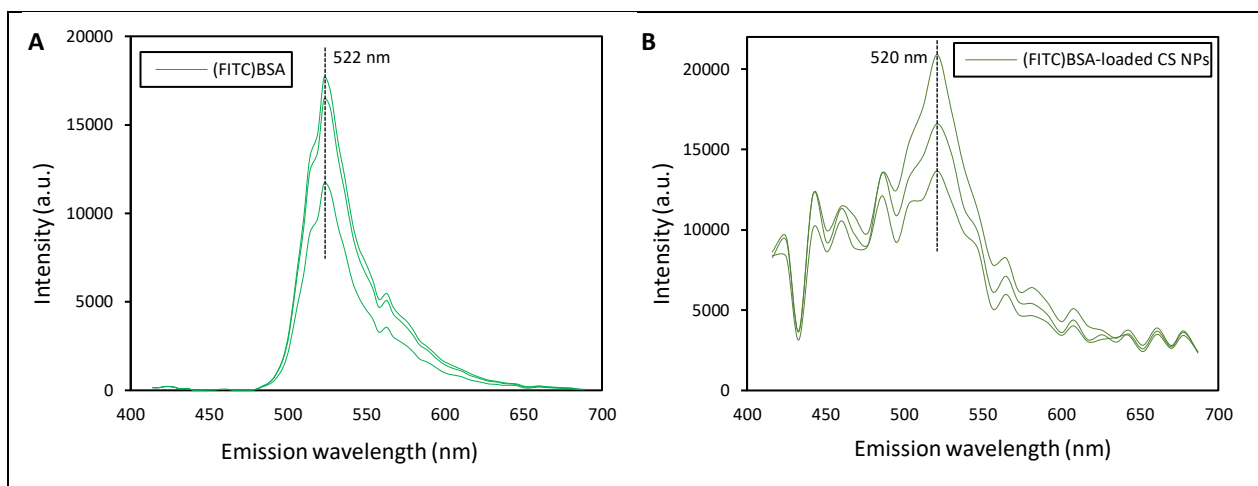


Figure 15. Fluorescence emission spectra of (A) FITC-conjugated BSA ((FITC)BSA) and (B) (FITC)BSA-loaded chitosan nanoparticles ((FITC)BSA-loaded CS NPs).

7.2.2. Encapsulation of recombinant porcine IFN α protein

Once the protein encapsulation within chitosan nanoparticles was achieved, this research moved forward to the encapsulation of the recombinant porcine interferon α for the design of an *in vitro* biologically active rpIFN α nanoparticle-based formulation. Hence, rpIFN α -loaded CS NPs were synthesized and characterized regarding their physicochemical and biological properties.

7.2.2.1. Size and size distribution characterization

Identical to the (FITC)BSA-loaded CS NPs synthesis procedure, 24 μ g of rpIFN α were added to the CS solution before the addition of the TPP in order to synthesize rpIFN α -loaded CS NPs. In this way, numerous batches of rpIFN α -loaded CS NPs were prepared and characterized regarding their hydrodynamic diameter and their PDI, through DLS. The results (**Figure 16**) showed that rpIFN α -loaded CS NPs owned an average hydrodynamic diameter and average PDI of 196.82 nm and 0.22, respectively. Similar to the case of CS NPs, statistical analyses demonstrated that the rpIFN α -loaded CS NPs were reproducibly synthesized using this ionotropic gelation-based procedure. Noteworthy, it was identified that 24 μ g of rpIFN α do not affect the formation mechanism of CS NPs; based on the fact that electrostatic interactions among rpIFN α , CS, and TPP did not provoke significant differences in the hydrodynamic diameter and PDI between rpIFN α -loaded CS NPs and CS NPs. Consequently, this finding revealed to the rpIFN α -loaded CS NPs as low polydisperse particles, with an average hydrodynamic diameter favorable to drug delivery applications (45). In this aspect, consistent with Danaei *et al.* (66), this preliminary study validated the feasibility of using rpIFN α -loaded CS NPs as a long-lasting protein nanoformulation.

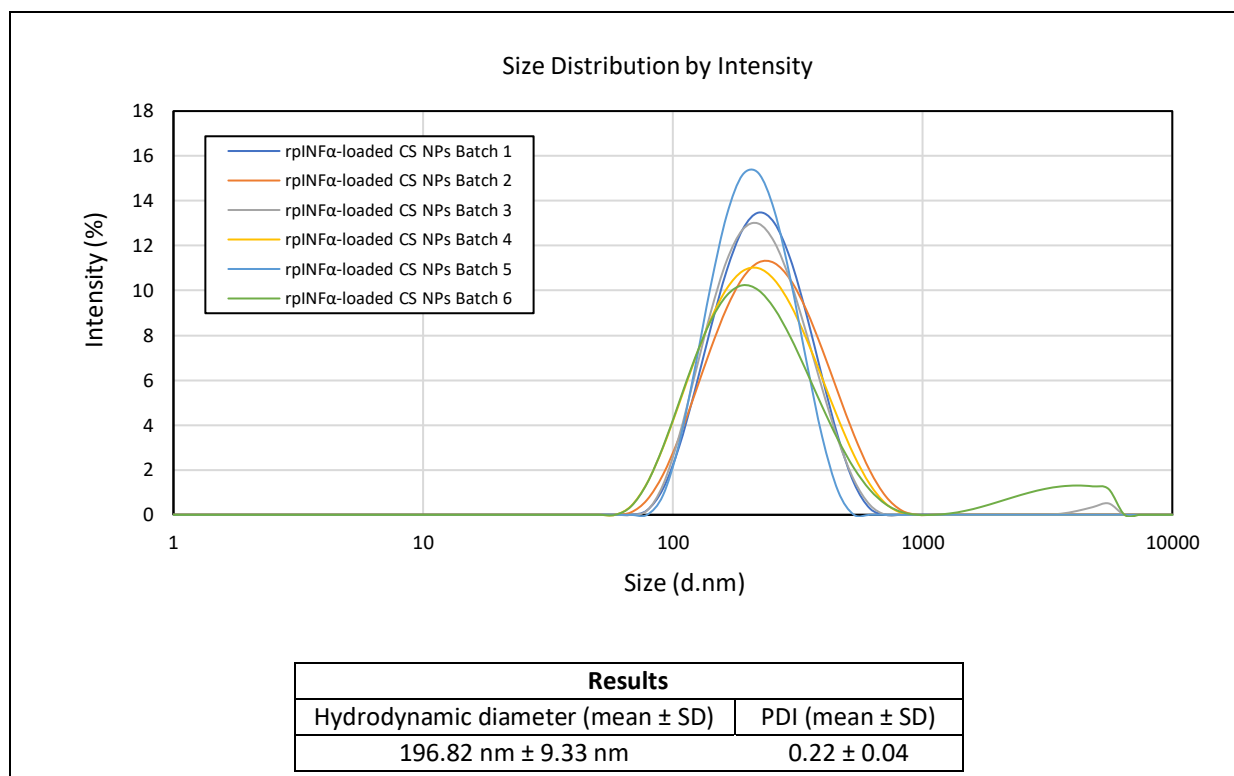


Figure 16. DLS characterization (size distribution by intensity) of rpIFN α -loaded chitosan nanoparticles. Results are indicated as mean \pm SD (n = 6).

7.2.2.2. Physical stability characterization

Comparable to CS NPs, ζ -potential was measured to evaluate the physical stability of rpIFN α -loaded CS NPs in colloidal suspension. As displayed in **Figure 17**, the ζ -potential distribution of rpIFN α -loaded CS NPs was found narrowly centered at +30.4 mV. Although slightly down-shifted in contrast to the ζ -potential distribution of CS NPs, rpIFN α -loaded CS NPs were also categorized as cationic particles with high stability in aqueous media, as reported in the literature (61). Consistent with Trapani *et al.* (133), this result suggested that positively charged CS chains mainly constituted the surface of rpIFN α -loaded CS NPs. At the same time, rpIFN α was trapped within the particle. Crucially, since electrostatic interactions between the cationic rpIFN α -loaded CS NPs and the anionic cell membranes are conceivable, the *in vivo* rpIFN α tissue- and cellular-permeability can be enhanced (96,133). As a consequence, this finding suggests that rpIFN α -loaded CS NPs could constitute promising protein delivery systems aimed at improving the pharmacological performance of rpIFN α formulations.

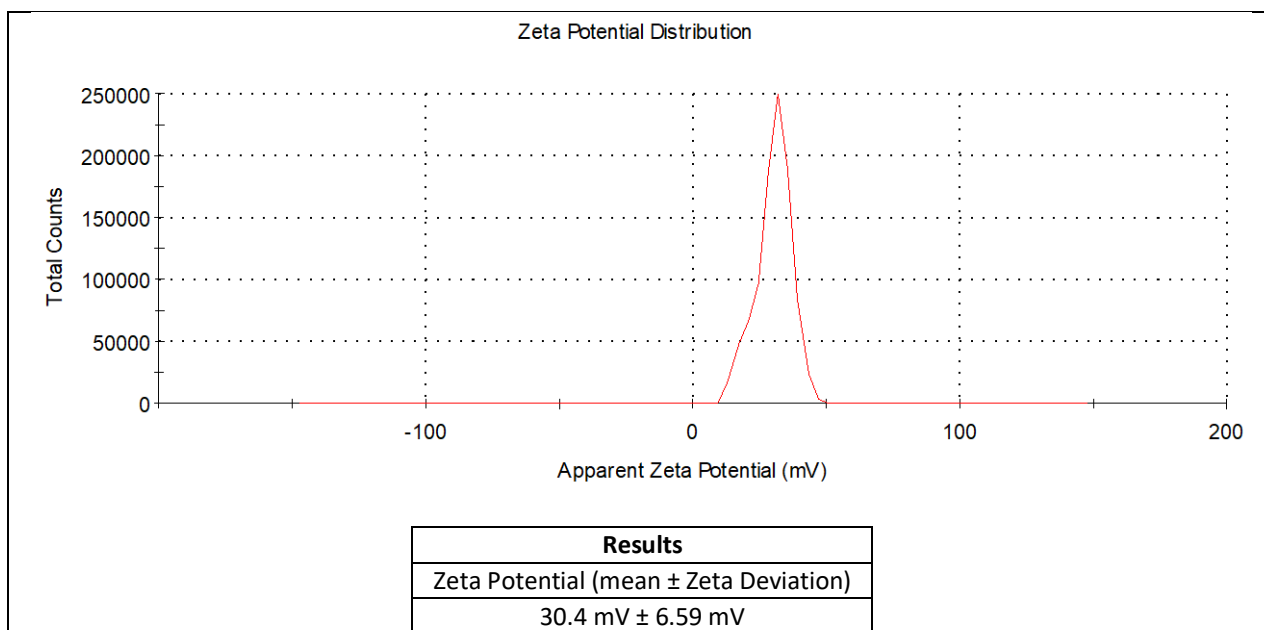


Figure 17. Zeta potential distribution of rpIFN α -loaded chitosan. Results are indicated as mean \pm Zeta Deviation.

7.2.2.3. Morphology characterization

Similar to CS NPs, the morphology of rpIFN α -loaded CS NPs was characterized using Transmission Electron Microscopy. TEM micrographs are shown in **Figure 18**. Likewise CS NPs, the results indicated that rpIFN α -loaded CS NPs were structured as solid particles with spherical morphology, which fits previously published findings (25). Also, there was a satisfactory consistency between the actual sizes of rpIFN α -loaded CS NPs and the above outlined DLS measurements. As noted in the literature review, the biological performance of nanoparticle-based protein formulations is tremendously affected by the size of nanocarriers; these nanoparticles should be of \sim 200 nm in diameter to get internalized by the cells, passively target tumor tissues, and stay in blood circulation for a long time (63). In this sense, TEM images offered compelling evidence about the high potential of rpIFN α -loaded CS NPs as a potent candidate for protein delivery purposes (108).

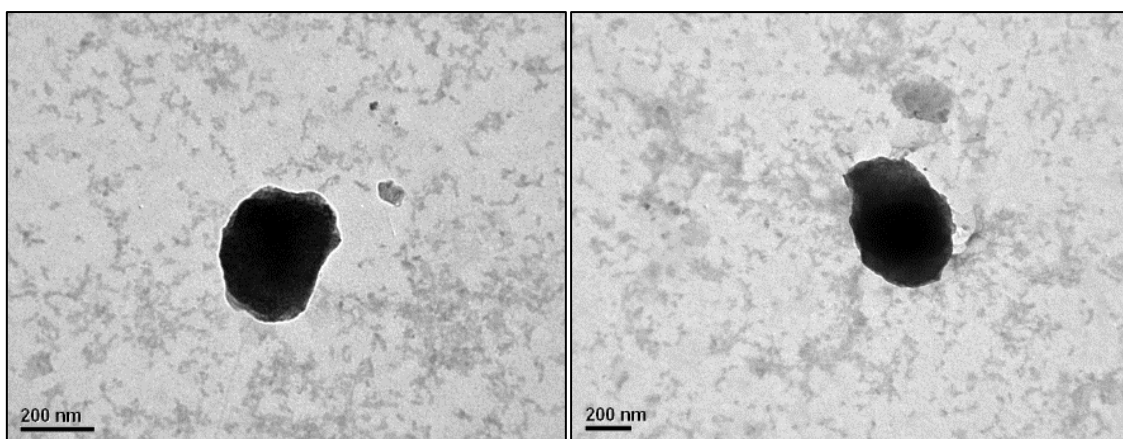


Figure 18. Transmission electron micrographs of rpIFN α -loaded CS NPs.

7.2.2.4. *In vitro* drug release kinetics profile

The drug release kinetics of rpIFN α -loaded CS NPs synthesized with 24 μ g of rpIFN α was studied *in vitro* during a period of 7 days in simulated physiological conditions. The cumulative release profile of rpIFN α (**Figure 19**) was analytically tracked using the Thermo Scientific™ Micro BCA™ Protein Assay Kit. Despite the limitations of this protein quantification method concomitantly with the interference in the protein concentration measurements provoked by chitosan polymer chains (117), the protein release profile of rpIFN α -loaded CS NPs was significantly ($p < 0.05$) differentiated from the control (CS NPs). Thus, the results described a sustained release of rpIFN α from the nanoparticles up to 171 h (more than 7 days).

Interestingly, the cumulative *in vitro* protein release profile of rpIFN α -loaded CS NPs did not show an initial burst release of protein. This means that neglectable amounts of protein were located on the surface of the particles while the release was due a slow degradation of the CS polymeric matrix (116). Therefore, this observation supported what was suggested by the ζ -potential results, i.e., rpIFN α -loaded CS NPs were stable, long-lasting protein delivery nanosystems, as stated by Du *et al.* (106) and Shi *et al.* (134).

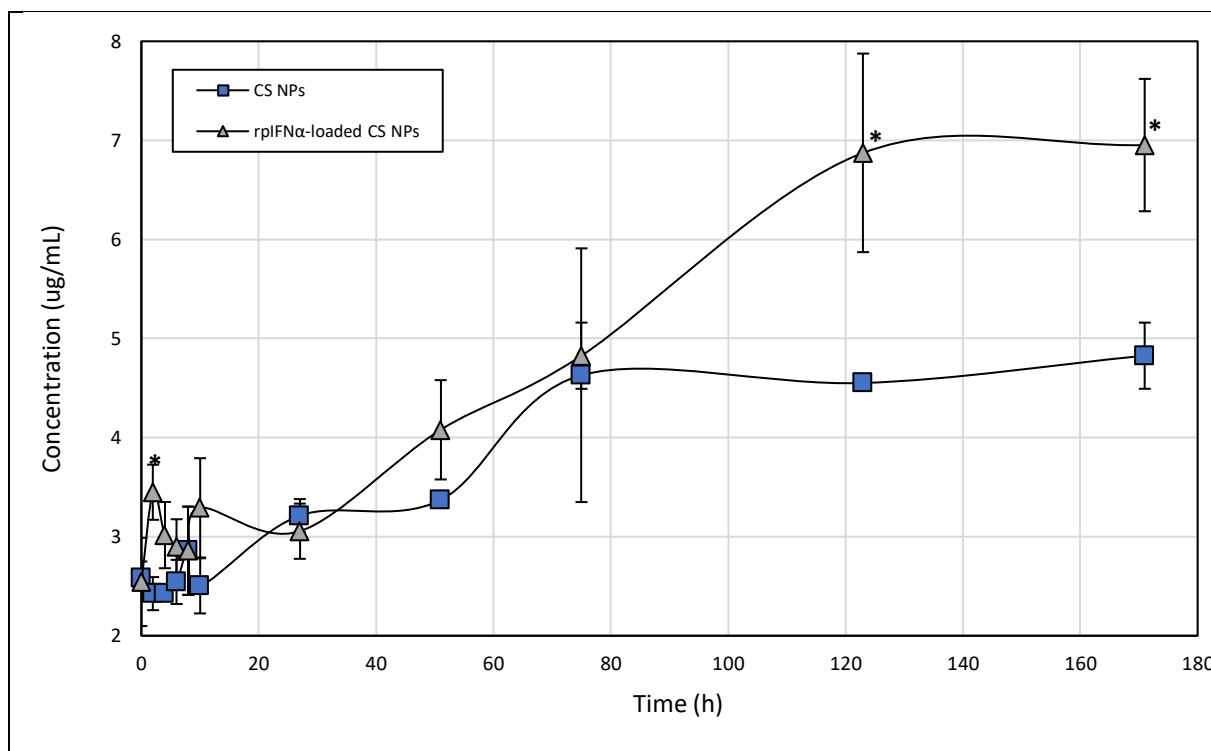


Figure 19. Cumulative *in vitro* protein release profile of chitosan nanoparticles and rpIFN α -loaded chitosan nanoparticles during 171 h. Results shown as mean \pm SD. * $p < 0.05$

7.3. Cell assays

7.3.1. Cell viability assay

The *in vitro* toxicological profile of CS NPs and rpIFN α -loaded CS NPs was evaluated on PK-15 cells by performing an MTT assay. As seen in **Figure 20**, both types of nanoparticles were assessed at different concentrations (0.2, 1, 2, and 10 mg/mL). Relatively to the untreated cells (control cells), the results did not find cell viability significantly lower at any of the examined conditions. Worth mentioning, the MTT assay is a colorimetric viability assay based on the quantification of the catabolic activity of the mitochondrial dehydrogenase enzyme, presented exclusively in metabolically active cells (135). Since the metabolic activity results of control cells and treated cells were similar, therefore CS NPs and rpIFN α -loaded CS NPs revealed not cytotoxic towards PK-15 cells under the studied conditions (116). Although further *in vivo* cytotoxicity studies need to be conducted in order to observe the actual safety of nanoparticles (24), this preliminary analysis revealed the CS NPs and rpIFN α -loaded CS NPs as being well tolerated by the cells (136). As a consequence, this study demonstrated that CS NPs and rpIFN α -loaded CS NPs were biocompatible systems suitable for the design of rpIFN α nanoformulation with therapeutic purposes (77).

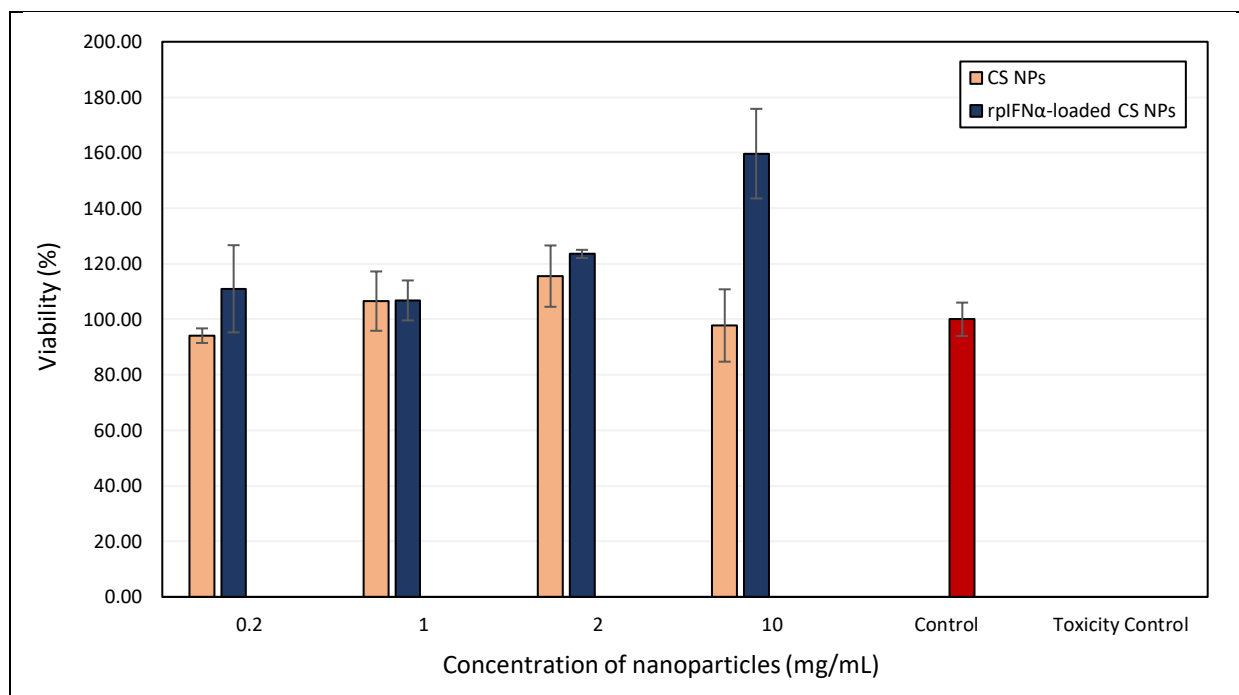


Figure 20. Viability of PK15 cells after the treatment with chitosan nanoparticles and rplIFN α -loaded chitosan nanoparticles, as measured by the MTT assay. Results are shown as mean \pm SD.

7.3.2. Cellular uptake of protein-loaded chitosan nanoparticles

Cellular uptake of the protein-loaded chitosan nanoparticles was studied *in vitro* using confocal microscopy. In this regard, HEp-2 cells were co-incubated with (FITC)BSA-loaded CS NPs synthesized with 240 μ g of (FITC)BSA for 24 h. Next, the nuclei and mitochondria of cells were stained using Hoechst 33342 and MitoTracker[®] Red CMXRos, respectively, in order to monitor the intracellular fate of (FITC)BSA-loaded CS NPs (63). As presented in **Figure 21**, the resulting confocal micrographs showed that the nanoparticles were localized inside the cells, specifically, in the cytoplasmic matrix. Consequently, in total agreement with He *et al.* (61) and Hu *et al.* (78), this assay confirmed the cellular uptake of (FITC)BSA-loaded CS NPs, 24 h post-incubation. Besides, it confirmed what was suggested by previous findings regarding the size, size distribution, surface charge, and morphology of CS NPs and protein-loaded CS NPs, i.e., protein-delivery nanosystems can be internalized by the cells. Finally, this observation offers evidence that these CS-based nanocarriers can be potentially exploited for the transporting of therapeutic agents intracellularly (13,56,63).

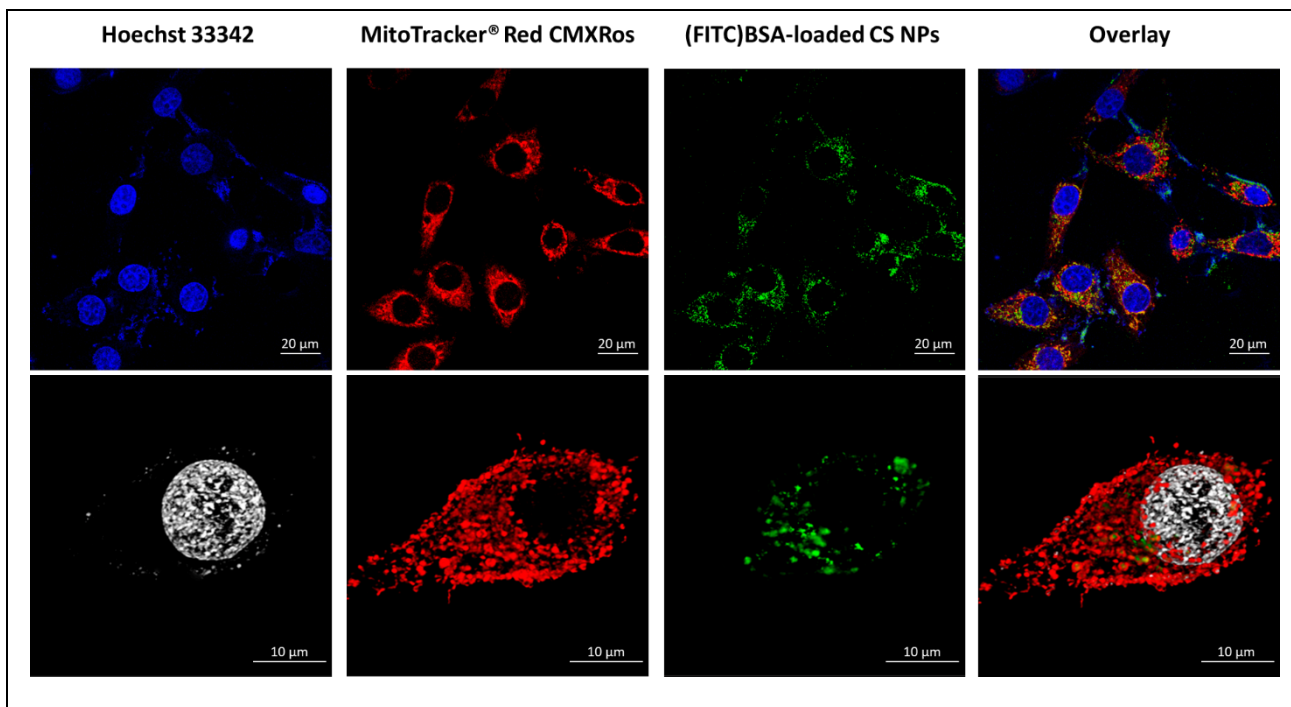


Figure 21. Confocal micrographs showing the localization of (FITC)BSA-loaded CS NPs in HEp-2 cells, 24 h post-incubation. As specified earlier, Hoechst 33342 and MitoTracker® Red CMXRos were used to label the nuclei and mitochondria of cells, respectively.

7.3.3. *In vitro* antiviral activity of the encapsulated rpIFN α

Biological activity of rpIFN α encapsulated in rpIFN α -loaded CS NPs was studied *in vitro* by evaluating its antiviral activity against Mengovirus in HEp-2 cells. For this study, the nanoparticles were synthesized using 240 μ g of rpIFN α . Once rpIFN α -loaded CS NPs were synthesized, their protein EE% was measured using SEC-HPLC. As a result, protein EE% was identified as being equal to 75%. Followed, protein release from rpIFN α -loaded CS NPs and CS NPs (control) was induced identically to the above-performed *in vitro* drug release kinetic characterization assay for 120 h. The resulting supernatants from the protein release induction were sampled at 3 different dates (0, 60, 120 h). Thus, the capability of the sampled supernatants to inhibit the cytopathic effect of Mengovirus in cells was quantified by comparing them with standardized commercial recombinant human IFN α (Heberon Alfa R®), as suggested by Meager (112).

As shown in **Figure 22**, all the samples of rpIFN α exhibited antiviral activity greater than 10^3 IU, while no significant antiviral activity was found with any sample of CS NPs. Contrary to expectations, antiviral activity was observed in the rpIFN α -loaded CS NPs supernatant sample at 0 h. However, as reported in previous works (24,84,108), this initial protein burst release was seemingly provoked by a simple process of protein desorption from the nanoparticle surface as a chunk of the 240 μ g of rpIFN α used for the NPs synthesis could have been retained on the particle surface.

Remarkably, the antiviral activity of encapsulated rpIFN α kept increasing for at least 5 days. Hence, this antiviral activity assay verified that the encapsulated rpIFN α remained active after its encapsulation and during its delivery from the CS polymeric matrix. Therefore, these encouraging results indicate that the encapsulation of rpIFN α in CS NPs may be used as a promising nanomedicine-based strategy to formulate rpIFN α . Accordingly, the presented rpIFN α -loaded CS NPs opens new horizons for the design of pharmacologically optimized rpIFN α therapeutics with veterinary purposes.

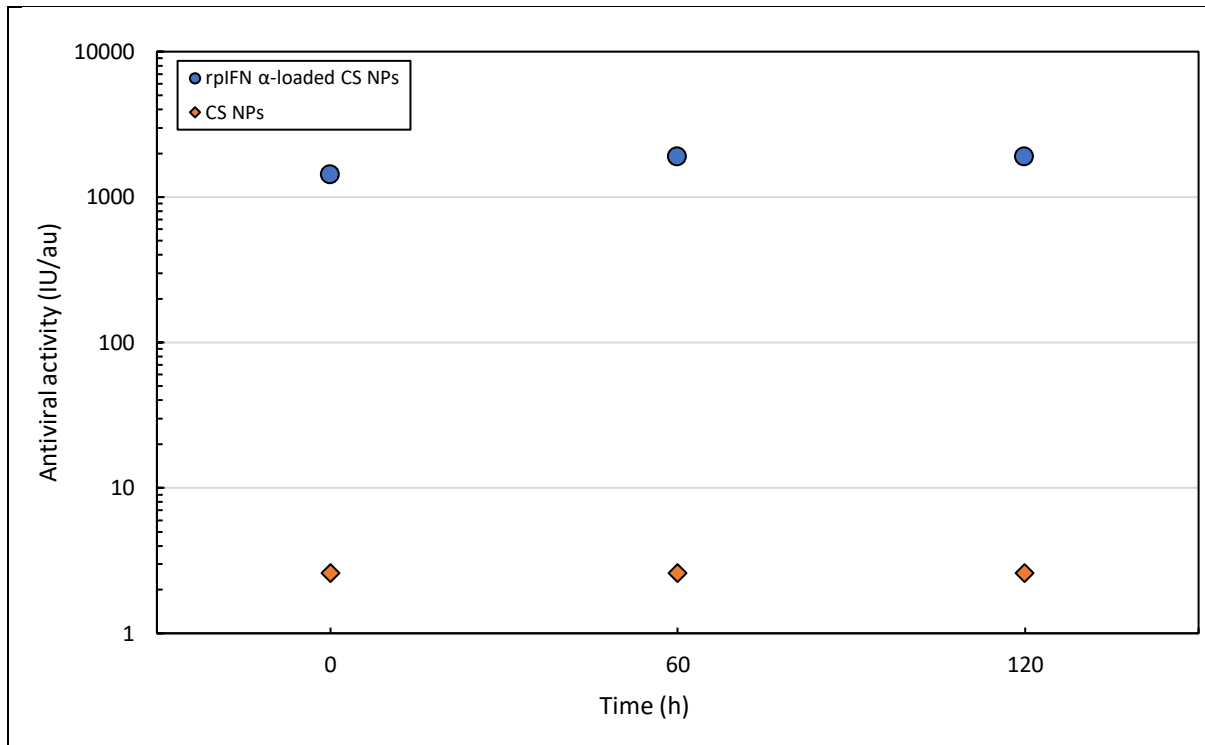


Figure 22. *In vitro* antiviral activity of rpIFN α against Mengovirus in Hep-2 cells.

Chapter V

8. Conclusions and Recommendations

Throughout this undergraduate thesis, it was described the design, synthesis, and characterization of a novel *in vitro* biologically active recombinant porcine IFN α formulation, assisted by chitosan nanoparticles. This work found reproducible the long-lasting protein delivery nanosystems attained via scalable ionotropic gelation reactions, between chitosan and tripolyphosphate. In detail, protein-loaded CS NPs were identified as highly stable and homogeneous spherical particles with an average size of ~200 nm. Structurally, CS-based nanocarriers were shown as being constituted by cationic CS polymer chains crosslinked by TPP, with the capacity to efficiently encapsulate proteins as well as steadily release them. Furthermore, it was observed that these protein-loaded CS NPs were prone to be taken up by cells. Finally, this research obtained satisfactory results demonstrating that rpIFN α conserves its antiviral activity *in vitro* after its encapsulation and subsequent release from the CS polymeric matrix.

Taken together, these findings validate the feasibility of protein-loaded CS NPs for the design of pIFN α formulations with optimized *in vivo* pharmacological performance in veterinary purposes. Besides, these results suggest that CS-based nanocarriers might be adapted to the encapsulation of a broad list of labile therapeutic agents for the development of novel therapeutics.

The results of this investigation are encouraging; however, all the data presented here come from *in vitro* studies and, consequently, lack the presence of systemic biological environments, which could alter the pharmacological performance of these nanoformulations. Therefore, the pharmacokinetic properties of pIFN α -loaded CS NPs should be further validated by *in vivo* animal studies.

Bibliography

1. Leader B, Baca QJ, Golan DE. Protein therapeutics: a summary and pharmacological classification. *Nat Rev Drug Discov* [Internet]. 2008 Jan;7(1):21–39. Available from: <http://www.nature.com/articles/nrd2399>
2. Usmani SS, Bedi G, Samuel JS, Singh S, Kalra S, Kumar P, et al. THPdb: Database of FDA-approved peptide and protein therapeutics. Sang Q-XA, editor. *PLoS One* [Internet]. 2017 Jul 31;12(7). Available from: <https://dx.plos.org/10.1371/journal.pone.0181748>
3. Lagassé HAD, Alexaki A, Simhadri VL, Katagiri NH, Jankowski W, Sauna ZE, et al. Recent advances in (therapeutic protein) drug development. *F1000Research* [Internet]. 2017 Feb 7;6:113. Available from: <https://f1000research.com/articles/6-113/v1>
4. Pandey GS, Sauna ZE. Pharmacogenetics and the Immunogenicity of Protein Therapeutics. *J Interf Cytokine Res* [Internet]. 2014 Dec;34(12):931–7. Available from: <http://www.liebertpub.com/doi/10.1089/jir.2012.0136>
5. Yanover C, Jain N, Pierce G, Howard TE, Sauna ZE. Pharmacogenetics and the immunogenicity of protein therapeutics. *Nat Biotechnol* [Internet]. 2011 Oct 13;29(10):870–3. Available from: <http://www.nature.com/articles/nbt.2002>
6. Kintzing JR, Filsinger Interrante M V., Cochran JR. Emerging Strategies for Developing Next-Generation Protein Therapeutics for Cancer Treatment [Internet]. Vol. 37, *Trends in Pharmacological Sciences*. Elsevier Ltd; 2016. p. 993–1008. Available from: <http://dx.doi.org/10.1016/j.tips.2016.10.005>
7. Zhang L, Gu F, Chan J, Wang A, Langer R, Farokhzad O. Nanoparticles in Medicine: Therapeutic Applications and Developments. *Clin Pharmacol Ther* [Internet]. 2008 May 24;83(5):761–9. Available from: <http://doi.wiley.com/10.1038/sj.clpt.6100400>
8. Alexis F, Rhee J, Richie JP, Radovic-Moreno AF, Langer R, Farokhzad OC. New frontiers in nanotechnology for cancer treatment. *Urol Oncol Semin Orig Investig* [Internet]. 2008 Jan;26(1):74–85. Available from: <https://linkinghub.elsevier.com/retrieve/pii/S1078143907000920>
9. Sainz V, Connot J, Matos AI, Peres C, Zupančič E, Moura L, et al. Regulatory aspects on nanomedicines. Vol. 468, *Biochemical and Biophysical Research Communications*. 2015. p. 504–10.
10. Pridgen EM, Alexis F, Farokhzad OC. Polymeric nanoparticle drug delivery technologies for oral delivery applications. *Expert Opin Drug Deliv* [Internet]. 2015 Sep 2;12(9):1459–73. Available from: <http://www.tandfonline.com/doi/full/10.1517/17425247.2015.1018175>
11. Elsabahy M, Wooley KL. Design of polymeric nanoparticles for biomedical delivery

- applications. *Chem Soc Rev* [Internet]. 2012;41(7):2545–61. Available from: <http://xlink.rsc.org/?DOI=c2cs15260f>
12. Mohammed MA, Syeda JTM, Wasan KM, Wasan EK. An overview of chitosan nanoparticles and its application in non-parenteral drug delivery. Vol. 9, *Pharmaceutics*. 2017.
 13. Wang JJ, Zeng ZW, Xiao RZ, Xie T, Zhou GL, Zhan XR, et al. Recent advances of chitosan nanoparticles as drug carriers. Vol. 6, *International journal of nanomedicine*. 2011. p. 765–74.
 14. Divya K, Jisha MS. Chitosan nanoparticles preparation and applications. *Environ Chem Lett*. 2018;16(1):101–12.
 15. Ali A, Ahmed S. A review on chitosan and its nanocomposites in drug delivery [Internet]. Vol. 109, *International Journal of Biological Macromolecules*. Elsevier B.V.; 2018. p. 273–86. Available from: <http://dx.doi.org/10.1016/j.ijbiomac.2017.12.078>
 16. Pestka S, Krause CD, Walter MR. Interferons, interferon-like cytokines, and their receptors. *Immunol Rev*. 2004;202:8–32.
 17. Lesinski GB, Sharma S, Varker KA, Sinha P, Ferrari M, Carson WE. Release of biologically functional interferon-alpha from a nanochannel delivery system. *Biomed Microdevices*. 2005;7(1):71–9.
 18. De Castro FA, Bonini Palma PV, Morais FR, Simões BP, Carvalho PVB, Ismael SJ, et al. Immunological effects of interferon-alpha on chronic myelogenous leukemia. *Leuk Lymphoma*. 2003;44(12):2061–7.
 19. Liu L, Fan W, Zhang H, Zhang S, Cui L, Wang M, et al. Interferon as a Mucosal Adjuvant for an Influenza Vaccine in Pigs. *Virol Sin* [Internet]. 2019;34(3):324–33. Available from: <https://doi.org/10.1007/s12250-019-00102-7>
 20. Yu HY, Qu MS, Zhang JL, Gan L, Zhao Y, Shan XQ, et al. Recombinant Porcine Interferon Alpha Enhances Immune Responses to Killed Porcine Reproductive and Respiratory Syndrome Virus Vaccine in Pigs. *Viral Immunol*. 2019;32(9):383–92.
 21. Lefevre F, L'Haridon R, Borrás-Cuesta F, La Bonnardiere C. Production, purification and biological properties of an Escherichia coli-derived recombinant porcine alpha interferon. *J Gen Virol*. 1990;71(5):1057–63.
 22. Du J, Luo J, Yu J, Mao X, Luo Y, Zheng P, et al. Manipulation of Intestinal Antiviral Innate Immunity and Immune Evasion Strategies of Porcine Epidemic Diarrhea Virus. *Biomed Res Int*. 2019;2019.
 23. Feczko T, Fodor-Kardos A, Sivakumaran M, Haque Shubhra QT. In vitro IFN- α release from IFN- α - and pegylated IFN- α -loaded poly(lactic-co-glycolic acid) and pegylated poly(lactic-co-glycolic acid) nanoparticles. *Nanomedicine* [Internet]. 2016 Aug;11(16):2029–34. Available from: <https://www.futuremedicine.com/doi/10.2217/nnm-2016-0058>
 24. Li S, Zhao B, Wang F, Wang M, Xie S, Wang S, et al. Yak interferon-alpha loaded solid lipid nanoparticles for controlled release. *Res Vet Sci* [Internet]. 2010;88(1):148–53. Available

- from: <http://dx.doi.org/10.1016/j.rvsc.2009.06.010>
25. Cánepa C, Imperiale JC, Berini CA, Lewicki M, Sosnik A, Biglione MM. Development of a Drug Delivery System Based on Chitosan Nanoparticles for Oral Administration of Interferon- α . *Biomacromolecules*. 2017;18(10):3302–9.
 26. Zong Y, Tan X, Xiao J, Zhang X, Xia X, Sun H. Half-life extension of porcine interferon- α by fusion to the IgG-binding domain of streptococcal G protein. *Protein Expr Purif* [Internet]. 2019;153(June 2018):53–8. Available from: <https://doi.org/10.1016/j.pep.2018.08.012>
 27. Bernard I, Castelain S, Charleston B, Fray MD, Capiod J, Duverlie G. Quantification of Different Human Alpha Interferon Subtypes and Pegylated Interferon Activities by Measuring MxA Promoter Activation. *Antimicrob Agents Chemother*. 2005;49(9):3770–5.
 28. Ventola CL. Progress in Nanomedicine: Approved and Investigational Nanodrugs. P T [Internet]. 2017 Dec;42(12):742–55. Available from: <http://www.ncbi.nlm.nih.gov/pubmed/29234213>
 29. Lobatto ME, Fuster V, Fayad ZA, Mulder WJM. Perspectives and opportunities for nanomedicine in the management of atherosclerosis. *Nat Rev Drug Discov*. 2011;10(11):835–52.
 30. Howard KA. Nanomedicine: Working Towards Defining the Field. In: Howard KA, Vorup-Jensen T, Peer D, editors. *Nanomedicine* [Internet]. New York, NY: Springer New York; 2016. p. 1–12. (Advances in Delivery Science and Technology). Available from: <http://link.springer.com/10.1007/978-1-4939-3634-2>
 31. Wagner V, Dullaart A, Bock AK, Zweck A. The emerging nanomedicine landscape. *Nat Biotechnol*. 2006;24(10):1211–7.
 32. Jain KK. Nanomedicine: Application of nanobiotechnology in medical practice. *Med Princ Pract*. 2008;17(2):89–101.
 33. Wu LP, Wang D, Li Z. Grand challenges in nanomedicine. *Mater Sci Eng C* [Internet]. 2020;106(August 2018):110302. Available from: <https://doi.org/10.1016/j.msec.2019.110302>
 34. Farooq MA, Aquib M, Farooq A, Haleem Khan D, Joelle Maviah MB, Sied Filli M, et al. Recent progress in nanotechnology-based novel drug delivery systems in designing of cisplatin for cancer therapy: an overview. *Artif Cells, Nanomedicine Biotechnol* [Internet]. 2019;47(1):1674–92. Available from: <https://doi.org/10.1080/21691401.2019.1604535>
 35. Sandra F, Khaliq NU, Sunna A, Care A. Developing Protein-Based Nanoparticles as Versatile Delivery Systems for Cancer Therapy and Imaging. *Nanomaterials* [Internet]. 2019 Sep 16;9(9):1329. Available from: <https://www.mdpi.com/2079-4991/9/9/1329>
 36. Yadav HKS, Almokdad AA, Shaluf SIM, Debe MS. Polymer-Based Nanomaterials for Drug-Delivery Carriers. In: *Nanocarriers for Drug Delivery* [Internet]. Elsevier Inc.; 2019. p. 531–56. Available from: <http://dx.doi.org/10.1016/B978-0-12-814033-8.00017-5>
 37. Sahoo SK, Parveen S, Panda JJ. The present and future of nanotechnology in human health

- care. *Nanomedicine Nanotechnology, Biol Med.* 2007;3(1):20–31.
38. Shanmugapriya K, Kang HW. Engineering pharmaceutical nanocarriers for photodynamic therapy on wound healing: Review. *Mater Sci Eng C* [Internet]. 2019;105(September 2018):110110. Available from: <https://doi.org/10.1016/j.msec.2019.110110>
 39. Venugopal I, Mehta AI, Linninger AA. Drug Delivery Applications of Nanoparticles in the Spine. In: *Methods in Molecular Biology* [Internet]. 2020. p. 121–43. Available from: http://link.springer.com/10.1007/978-1-4939-9798-5_5
 40. Underwood C, van Eps AW. Nanomedicine and veterinary science: The reality and the practicality. *Vet J* [Internet]. 2012;193(1):12–23. Available from: <http://dx.doi.org/10.1016/j.tvjl.2012.01.002>
 41. Saboktakin M. The biological and biomedical nanoparticles - synthesis and applications. *Adv Mater Sci.* 2017;2(3):1–14.
 42. Wachsmann P, Lamprecht A. Polymeric nanoparticles for the selective therapy of inflammatory bowel disease. In: *Methods in Enzymology* [Internet]. 1st ed. Elsevier Inc.; 2012. p. 377–97. Available from: <http://dx.doi.org/10.1016/B978-0-12-391860-4.00019-7>
 43. Lu XY, Wu DC, Li ZJ, Chen GQ. Polymer nanoparticles. In: *Progress in Molecular Biology and Translational Science* [Internet]. 1st ed. Elsevier Inc.; 2011. p. 299–323. Available from: <http://dx.doi.org/10.1016/B978-0-12-416020-0.00007-3>
 44. Liu S, Maheshwari R, Kiick KL. Polymer-Based Therapeutics. *Macromolecules* [Internet]. 2009 Jan 13;42(1):3–13. Available from: <https://pubs.acs.org/doi/10.1021/ma801782q>
 45. Vasile C. Polymeric Nanomaterials: Recent Developments, Properties and Medical Applications [Internet]. *Polymeric Nanomaterials in Nanotherapeutics.* Elsevier Inc.; 2019. 1–66 p. Available from: <http://dx.doi.org/10.1016/B978-0-12-813932-5.00001-7>
 46. Wang Y, Li P, Tran TTD, Zhang J, Kong L. Manufacturing techniques and surface engineering of polymer based nanoparticles for targeted drug delivery to cancer. *Nanomaterials.* 2016;6(2).
 47. G. Nava-Arzaluz M, Pinon-Segundo E, Ganem-Rondero A, Lechuga-Ballesteros D. Single Emulsion-Solvent Evaporation Technique and Modifications for the Preparation of Pharmaceutical Polymeric Nanoparticles. *Recent Pat Drug Deliv Formul.* 2012;6(3):209–23.
 48. Mallakpour S, Behranvand V. Polymeric nanoparticles: Recent development in synthesis and application. *Express Polym Lett.* 2016;10(11):895–913.
 49. Patra JK, Das G, Fraceto LF, Campos EVR, Rodriguez-Torres MDP, Acosta-Torres LS, et al. Nano based drug delivery systems: Recent developments and future prospects. *J Nanobiotechnology* [Internet]. 2018;16(1):1–33. Available from: <https://doi.org/10.1186/s12951-018-0392-8>
 50. Xu S, Cui F, Huang D, Zhang D, Zhu A, Sun X, et al. PD-11 monoclonal antibody-conjugated nanoparticles enhance drug delivery level and chemotherapy efficacy in gastric cancer cells.

- Int J Nanomedicine. 2019;14:17–32.
51. Girija AR. Medical Applications of Polymer/Functionalized Nanoparticle Systems. In: Polymer Composites with Functionalized Nanoparticles [Internet]. Elsevier Inc.; 2019. p. 381–404. Available from: <http://dx.doi.org/10.1016/B978-0-12-814064-2.00012-3>
 52. Thomas S, Ninan N, Mohan S, Francis E. Natural polymers, biopolymers, biomaterials, and their composites, blends and IPNs. Natural Polymers, Biopolymers, Biomaterials, and Their Composites, Blends, and IPNs. 2012. 1–407 p.
 53. Lohcharoenkal W, Wang L, Chen YC, Rojanasakul Y. Protein Nanoparticles as Drug Delivery Carriers for Cancer Therapy. Biomed Res Int [Internet]. 2014;2014:1–12. Available from: <http://www.hindawi.com/journals/bmri/2014/180549/>
 54. Liu Y, Shi L, Su L, Van der Mei HC, Jutte PC, Ren Y, et al. Nanotechnology-based antimicrobials and delivery systems for biofilm-infection control. Chem Soc Rev. 2019;48(2):428–46.
 55. Patel BK, Parikh RH, Aboti PS. Development of Oral Sustained Release Rifampicin Loaded Chitosan Nanoparticles by Design of Experiment. J Drug Deliv. 2013;2013(May 2014):1–10.
 56. Biswas A, Shukla A, Maiti P. Biomaterials for Interfacing Cell Imaging and Drug Delivery: An Overview. Langmuir. 2019;
 57. Nikolić V, Ilić-Stojanović S, Petrović S, Tačić A, Nikolić L. Administration Routes for Nano Drugs and Characterization of Nano Drug Loading. In: Characterization and Biology of Nanomaterials for Drug Delivery. 2019. p. 587–625.
 58. Rivera Gil P, Hühn D, del Mercato LL, Sasse D, Parak WJ. Nanopharmacy: Inorganic nanoscale devices as vectors and active compounds. Pharmacol Res. 2010;62(2):115–25.
 59. Rawal M, Singh A, Amiji MM. Quality-by-Design Concepts to Improve Nanotechnology-Based Drug Development. Pharm Res. 2019;36(11):1–20.
 60. Xu R. Progress in nanoparticles characterization: Sizing and zeta potential measurement. Particuology [Internet]. 2008 Apr;6(2):112–5. Available from: <https://linkinghub.elsevier.com/retrieve/pii/S1674200108000357>
 61. He C, Yin L, Tang C, Yin C. Size-dependent absorption mechanism of polymeric nanoparticles for oral delivery of protein drugs. Biomaterials [Internet]. 2012;33(33):8569–78. Available from: <http://dx.doi.org/10.1016/j.biomaterials.2012.07.063>
 62. Gustafson HH, Holt-Casper D, Grainger DW, Ghandehari H. Nanoparticle uptake: The phagocyte problem. Nano Today [Internet]. 2015 Aug;10(4):487–510. Available from: <https://www.ncbi.nlm.nih.gov/pmc/articles/PMC4666556/pdf/nihms707252.pdf>
 63. Damiati S, Scheberl A, Zayni S, Damiati SA, Schuster B, Kompella UB. Albumin-bound nanodiscs as delivery vehicle candidates: Development and characterization. Biophys Chem [Internet]. 2019;251(April):106178. Available from: <https://doi.org/10.1016/j.bpc.2019.106178>

64. Turecek PL, Bossard MJ, Schoetens F, Ivens IA. PEGylation of Biopharmaceuticals: A Review of Chemistry and Nonclinical Safety Information of Approved Drugs [Internet]. Vol. 105, *Journal of Pharmaceutical Sciences*. Elsevier Ltd; 2016. p. 460–75. Available from: <http://dx.doi.org/10.1016/j.xphs.2015.11.015>
65. Huang M, Khor E, Lim L-Y. Uptake and Cytotoxicity of Chitosan Molecules and Nanoparticles: Effects of Molecular Weight and Degree of Deacetylation. *Pharm Res* [Internet]. 2004 Feb;21(2):344–53. Available from: <http://link.springer.com/10.1023/B:PHAM.0000016249.52831.a5>
66. Danaei M, Dehghankhold M, Ataei S, Hasanzadeh Davarani F, Javanmard R, Dokhani A, et al. Impact of particle size and polydispersity index on the clinical applications of lipidic nanocarrier systems. *Pharmaceutics*. 2018;10(2):1–17.
67. Instruments Malvern. Dynamic Light Scattering Common Terms Defined. Malvern Guid [Internet]. 2011;1–6. Available from: www.malvern.com
68. Zhang L, Kosaraju SL. Biopolymeric delivery system for controlled release of polyphenolic antioxidants. *Eur Polym J*. 2007;43(7):2956–66.
69. Antoniou J, Liu F, Majeed H, Qi J, Yokoyama W, Zhong F. Physicochemical and morphological properties of size-controlled chitosan–tripolyphosphate nanoparticles. *Colloids Surfaces A Physicochem Eng Asp* [Internet]. 2015 Jan;465:137–46. Available from: <https://linkinghub.elsevier.com/retrieve/pii/S092777571400819X>
70. Desfrancois C, Auzély R, Texier I. Lipid nanoparticles and their hydrogel composites for drug delivery: A review. Vol. 11, *Pharmaceutics*. 2018.
71. Dogan Ü, Çiftçi H, Cetin D, Suludere Z, Tamer U. Nanoparticle embedded chitosan film for agglomeration free TEM images. *Microsc Res Tech*. 2017;80(2):163–6.
72. Newton AMJ, Kaur S. Solid lipid nanoparticles for skin and drug delivery. In: *Nanoarchitectonics in Biomedicine* [Internet]. Elsevier Inc.; 2019. p. 295–334. Available from: <http://dx.doi.org/10.1016/B978-0-12-816200-2.00015-3>
73. Enescu D, Cerqueira MA, Fucinos P, Pastrana LM. Recent advances and challenges on applications of nanotechnology in food packaging. A literature review. *Food Chem Toxicol* [Internet]. 2019;134(May):110814. Available from: <https://doi.org/10.1016/j.fct.2019.110814>
74. Nemati Y, Zahedi P, Baghdadi M, Ramezani S. Microfluidics combined with ionic gelation method for production of nanoparticles based on thiol-functionalized chitosan to adsorb Hg (II) from aqueous solutions. *J Environ Manage* [Internet]. 2019 May;238(October 2018):166–77. Available from: <https://doi.org/10.1016/j.jenvman.2019.02.124>
75. Ahmad M, Mudgil P, Gani A, Hamed F, Masoodi FA, Maqsood S. Nano-encapsulation of catechin in starch nanoparticles: Characterization, release behavior and bioactivity retention during simulated in-vitro digestion. *Food Chem* [Internet]. 2019;270:95–104. Available from: <https://doi.org/10.1016/j.foodchem.2018.07.024>

76. Bodnar M, Hartmann JF, Borbely J. Preparation and characterization of chitosan-based nanoparticles. *Biomacromolecules*. 2005;6(5):2521–7.
77. Shariatinia Z. Pharmaceutical applications of chitosan. *Adv Colloid Interface Sci* [Internet]. 2019 Jan;263:131–94. Available from: <https://doi.org/10.1016/j.cis.2018.11.008>
78. Hu CS, Chiang CH, Hong P Da, Yeh MK. Influence of charge on FITC-BSA-loaded chondroitin sulfate-chitosan nanoparticles upon cell uptake in human Caco-2 cell monolayers. *Int J Nanomedicine*. 2012;7:4861–72.
79. Luo Y, Zhang B, Cheng WH, Wang Q. Preparation, characterization and evaluation of selenite-loaded chitosan/TPP nanoparticles with or without zein coating. *Carbohydr Polym* [Internet]. 2010;82(3):942–51. Available from: <http://dx.doi.org/10.1016/j.carbpol.2010.06.029>
80. Katas H, Raja MAG, Lam KL. Development of chitosan nanoparticles as a stable drug delivery system for protein/siRNA. *Int J Biomater*. 2013;2013.
81. Zhang W. Nanoparticle Aggregation: Principles and Modeling. In: *Nanomaterial, Advances in Experimental Medicine and Biology* [Internet]. 2014. p. 19–43. Available from: http://link.springer.com/10.1007/978-94-017-8739-0_2
82. Delgado AV, González-Caballero F, Hunter RJ, Koopal LK, Lyklema J. Measurement and interpretation of electrokinetic phenomena. *J Colloid Interface Sci* [Internet]. 2007 May;309(2):194–224. Available from: <https://linkinghub.elsevier.com/retrieve/pii/S002197970700015X>
83. Nasti A, Zaki NM, De Leonardis P, Ungphaiboon S, Sansongsak P, Rimoli MG, et al. Chitosan/TPP and chitosan/TPP-hyaluronic acid nanoparticles: Systematic optimisation of the preparative process and preliminary biological evaluation. *Pharm Res*. 2009;26(8):1918–30.
84. Bugnicourt L, Ladavière C. Interests of chitosan nanoparticles ionically cross-linked with tripolyphosphate for biomedical applications [Internet]. Vol. 60, *Progress in Polymer Science*. Elsevier Ltd; 2016. p. 1–17. Available from: <http://dx.doi.org/10.1016/j.progpolymsci.2016.06.002>
85. Brunetti A, Felice R Di. *Encyclopedia of Membranes* [Internet]. Drioli E, Giorno L, editors. *Encyclopedia of Membranes*. Berlin, Heidelberg: Springer Berlin Heidelberg; 2016. Available from: <http://link.springer.com/10.1007/978-3-662-44324-8>
86. Albinali K, Zagho M, Deng Y, Elzatahry A. A perspective on magnetic core–shell carriers for responsive and targeted drug delivery systems. *Int J Nanomedicine* [Internet]. 2019 Mar;Volume 14:1707–23. Available from: <https://www.dovepress.com/a-perspective-on-magnetic-core-shell-carriers-for-responsive-and-targe-peer-reviewed-article-IJN>
87. Wong PT, Choi SK. Mechanisms of Drug Release in Nanotherapeutic Delivery Systems. *Chem Rev* [Internet]. 2015 May 13;115(9):3388–432. Available from: <https://pubs.acs.org/doi/10.1021/cr5004634>

88. D'Souza S. A Review of In Vitro Drug Release Test Methods for Nano-Sized Dosage Forms. *Adv Pharm.* 2014;2014:1–12.
89. Lu Y, Kim S, Park K. In vitro-in vivo correlation: Perspectives on model development. *Int J Pharm* [Internet]. 2011;418(1):142–8. Available from: <http://dx.doi.org/10.1016/j.ijpharm.2011.01.010>
90. Hillegass JM, Shukla A, Lathrop SA, MacPherson MB, Fukagawa NK, Mossman BT. Assessing nanotoxicity in cells in vitro. *Wiley Interdiscip Rev Nanomedicine Nanobiotechnology* [Internet]. 2010 May;2(3):219–31. Available from: <http://doi.wiley.com/10.1002/wnan.54>
91. Aslantürk ÖS. In Vitro Cytotoxicity and Cell Viability Assays: Principles, Advantages, and Disadvantages. In: *Genotoxicity - A Predictable Risk to Our Actual World* [Internet]. 2018. Available from: <http://dx.doi.org/10.5772/intechopen.71923>
92. Kong B, Seog JH, Graham LM, Lee SB. Experimental considerations on the cytotoxicity of nanoparticles. *Nanomedicine* [Internet]. 2011 Jul;6(5):929–41. Available from: <https://www.futuremedicine.com/doi/10.2217/nnm.11.77>
93. Salatin S, Yari Khosroushahi A. Overviews on the cellular uptake mechanism of polysaccharide colloidal nanoparticles. *J Cell Mol Med.* 2017;21(9):1668–86.
94. Hong SC, Yoo SY, Kim H, Lee J. Chitosan-based multifunctional platforms for local delivery of therapeutics. Vol. 15, *Marine Drugs*. 2017.
95. Yang P, Dong Y, Huang D, Zhu C, Liu H, Pan X, et al. Silk fibroin nanoparticles for enhanced bio-macromolecule delivery to the retina. *Pharm Dev Technol.* 2019;24(5):575–83.
96. Amidi M, Mastrobattista E, Jiskoot W, Hennink WE. Chitosan-based delivery systems for protein therapeutics and antigens. *Adv Drug Deliv Rev* [Internet]. 2010;62(1):59–82. Available from: <http://dx.doi.org/10.1016/j.addr.2009.11.009>
97. Venkatesan J, Anil S, Kim SK, Shim MS. Chitosan as a vehicle for growth factor delivery: Various preparations and their applications in bone tissue regeneration [Internet]. Vol. 104, *International Journal of Biological Macromolecules*. Elsevier B.V.; 2017. p. 1383–97. Available from: <http://dx.doi.org/10.1016/j.ijbiomac.2017.01.072>
98. Marpu S, Benton E. Shining Light on Chitosan: A Review on the Usage of Chitosan for Photonics and Nanomaterials Research. *Int J Mol Sci* [Internet]. 2018 Jun 17;19(6):1795. Available from: <http://www.mdpi.com/1422-0067/19/6/1795>
99. Liu C, Tan Y, Liu C, Chen X, Yu L. Preparations, characterizations and applications of Chitosan-based nanoparticles. *J Ocean Univ China.* 2007;6(3):237–43.
100. Mao S, Sun W, Kissel T. Chitosan-based formulations for delivery of DNA and siRNA. *Adv Drug Deliv Rev* [Internet]. 2010 Jan;62(1):12–27. Available from: <http://dx.doi.org/10.1016/j.addr.2009.08.004>
101. Ma Z, Garrido-Maestu A, Jeong KC. Application, mode of action, and in vivo activity of

- chitosan and its micro- and nanoparticles as antimicrobial agents: A review [Internet]. Vol. 176, Carbohydrate Polymers. Elsevier Ltd.; 2017. p. 257–65. Available from: <http://dx.doi.org/10.1016/j.carbpol.2017.08.082>
102. Fan W, Yan W, Xu Z, Ni H. Formation mechanism of monodisperse, low molecular weight chitosan nanoparticles by ionic gelation technique. *Colloids Surfaces B Biointerfaces* [Internet]. 2012;90(1):21–7. Available from: <http://dx.doi.org/10.1016/j.colsurfb.2011.09.042>
 103. Cheung RCF, Ng TB, Wong JH, Chan WY. Chitosan: An update on potential biomedical and pharmaceutical applications. Vol. 13, *Marine Drugs*. 2015. 5156–5186 p.
 104. Zhang Y, Sun T, Jiang C. Biomacromolecules as carriers in drug delivery and tissue engineering [Internet]. Vol. 8, *Acta Pharmaceutica Sinica B*. Elsevier B.V.; 2018. p. 34–50. Available from: <https://doi.org/10.1016/j.apsb.2017.11.005>
 105. Huang G, Liu Y, Chen L. Chitosan and its derivatives as vehicles for drug delivery. *Drug Deliv* [Internet]. 2017 Nov 10;24(2):108–13. Available from: <https://doi.org/10.1080/10717544.2017.1399305>
 106. Du Z, Liu J, Zhang T, Yu Y, Zhang Y, Zhai J, et al. A study on the preparation of chitosan-tripolyphosphate nanoparticles and its entrapment mechanism for egg white derived peptides. *Food Chem* [Internet]. 2019;286:530–6. Available from: <https://doi.org/10.1016/j.foodchem.2019.02.012>
 107. Sreekumar S, Goycoolea FM, Moerschbacher BM, Rivera-Rodriguez GR. Parameters influencing the size of chitosan-TPP nano- and microparticles. *Sci Rep*. 2018;8(1):1–11.
 108. Calvo P, Remuñán-López C, Vila-Jato JL, Alonso MJ. Novel hydrophilic chitosan-polyethylene oxide nanoparticles as protein carriers. *J Appl Polym Sci*. 1997;63(1):125–32.
 109. Othman N, Masarudin MJ, Kuen CY, Dasuan NA, Abdullah LC, Jamil SNAM. Synthesis and optimization of chitosan nanoparticles loaded with l-ascorbic acid and thymoquinone. *Nanomaterials*. 2018;8(11).
 110. Koukaras EN, Papadimitriou SA, Bikiaris DN, Froudakis GE. Insight on the formation of chitosan nanoparticles through ionotropic gelation with tripolyphosphate. *Mol Pharm*. 2012;9(10):2856–62.
 111. Zanotti C, Razzuoli E, Crooke H, Soule O, Pezzoni G, Ferraris M, et al. Differential biological activities of swine interferon- α subtypes. *J Interf Cytokine Res*. 2015;35(12):990–1002.
 112. Meager A. Biological assays for interferons. Vol. 261, *Journal of Immunological Methods*. 2002. p. 21–36.
 113. Carter WA. Mechanisms of cross-species activity of mammalian interferons. *Pharmacol Ther*. 1979;7(2):245–52.
 114. Stepensky D. Delivery of Peptides and Proteins to the Brain Using Nano-Drug Delivery Systems and Other Formulations. In: Howard KA, Vorup-Jensen T, Peer D, editors. *Nanomedicine* [Internet]. New York, NY: Springer New York; 2016. p. 201–20. (Advances in

- Delivery Science and Technology). Available from: http://link.springer.com/10.1007/978-1-4939-3634-2_9
115. Chaganti LK, Venkatakrishnan N, Bose K. An efficient method for FITC labelling of proteins using tandem affinity purification. *Biosci Rep*. 2018;38(6):1–8.
 116. Yeh MK, Cheng KM, Hu CS, Huang YC, Young JJ. Novel protein-loaded chondroitin sulfate-chitosan nanoparticles: Preparation and characterization. *Acta Biomater* [Internet]. 2011;7(10):3804–12. Available from: <http://dx.doi.org/10.1016/j.actbio.2011.06.026>
 117. Thermo Scientific™. Micro BCA Protein Assay Kit. Preparation of Standards and Working Reagent. 0747(23235).
 118. Jiang Y, Yu X, Su C, Zhao L, Shi Y. Chitosan nanoparticles induced the antitumor effect in hepatocellular carcinoma cells by regulating ROS-mediated mitochondrial damage and endoplasmic reticulum stress. *Artif Cells, Nanomedicine Biotechnol* [Internet]. 2019;47(1):747–56. Available from: <https://doi.org/10.1080/21691401.2019.1577876>
 119. Thermo Scientific™. Hoechst Stains. Mol Probes® Invit Detect Technol. 2005;(3):9–12.
 120. Thermo Scientific™. MitoTracker® Mitochondrion-Selective Probes. Mol Probes® Invit Detect Technol. 2008;
 121. Piras AM, Maisetta G, Sandreschi S, Esin S, Gazzarri M, Batoni G, et al. Preparation, physical-chemical and biological characterization of chitosan nanoparticles loaded with lysozyme. *Int J Biol Macromol* [Internet]. 2014;67:124–31. Available from: <http://dx.doi.org/10.1016/j.ijbiomac.2014.03.016>
 122. Azizi E, Namazi A, Haririan I, Fouladdel S, Khoshayand MR, Shotorbani PY, et al. Release profile and stability evaluation of optimized chitosan/alginate nanoparticles as EGFR antisense vector. *Int J Nanomedicine*. 2010;5(1):455–61.
 123. de Pinho Neves AL, Milioli CC, Müller L, Riella HG, Kuhnen NC, Stulzer HK. Factorial design as tool in chitosan nanoparticles development by ionic gelation technique. *Colloids Surfaces A Physicochem Eng Asp* [Internet]. 2014 Mar;445:34–9. Available from: <https://linkinghub.elsevier.com/retrieve/pii/S0927775713009758>
 124. Vimal S, Taju G, Nambi KSN, Abdul Majeed S, Sarath Babu V, Ravi M, et al. Synthesis and characterization of CS/TPP nanoparticles for oral delivery of gene in fish. *Aquaculture* [Internet]. 2012;358–359:14–22. Available from: <http://dx.doi.org/10.1016/j.aquaculture.2012.06.012>
 125. Bangun H, Tandiono S, Arianto A. Preparation and evaluation of chitosan-tripolyphosphate nanoparticles suspension as an antibacterial agent. *J Appl Pharm Sci*. 2018;8(12):147–56.
 126. Carey FA, Giuliano RM. Organic Chemistry [Internet]. 10th ed. Organic Chemistry. McGraw-Hill Education; 2017. Available from: <https://www.taylorfrancis.com/books/9781466559783>
 127. Socrates G. Infrared and Raman characteristic group frequencies, third edition. John Wiley & Sons, LTD. 2001.

128. Mayo D, Miller F, Hannah R. Course Notes on the Interpretation of Infrared and Raman Spectra. *Appl Spectrosc* [Internet]. 2004 Nov 30;583. Available from: <http://journals.sagepub.com/doi/10.1366/0003702042475583>
129. Henao E, Delgado E, Contreras H, Quintana G. Polyelectrolyte Complexation versus Ionotropic Gelation for Chitosan-Based Hydrogels with Carboxymethylcellulose, Carboxymethyl Starch, and Alginic Acid. *Int J Chem Eng*. 2018;2018.
130. Gan Q, Wang T, Cochrane C, McCarron P. Modulation of surface charge, particle size and morphological properties of chitosan-TPP nanoparticles intended for gene delivery. *Colloids Surfaces B Biointerfaces*. 2005;44(2–3):65–73.
131. Gao P, Xia G, Bao Z, Feng C, Cheng X, Kong M, et al. Chitosan based nanoparticles as protein carriers for efficient oral antigen delivery. *Int J Biol Macromol* [Internet]. 2016;91:716–23. Available from: <http://dx.doi.org/10.1016/j.ijbiomac.2016.06.015>
132. Hermanson GT. Fluorescent Probes. In: *Bioconjugate Techniques* [Internet]. Elsevier; 2013. p. 395–463. Available from: <https://linkinghub.elsevier.com/retrieve/pii/B9780123822390000108>
133. Trapani A, De Giglio E, Cafagna D, Denora N, Agrimi G, Cassano T, et al. Characterization and evaluation of chitosan nanoparticles for dopamine brain delivery. *Int J Pharm* [Internet]. 2011;419(1–2):296–307. Available from: <http://dx.doi.org/10.1016/j.ijpharm.2011.07.036>
134. Shi Y, Wan A, Shi Y, Zhang Y, Chen Y. Experimental and mathematical studies on the drug release properties of aspirin loaded chitosan nanoparticles. *Biomed Res Int* [Internet]. 2014;2014:1–8. Available from: <http://dx.doi.org/10.1155/2014/613619>
135. Kumar SP, Birundha K, Kaveri K, Devi KTR. Antioxidant studies of chitosan nanoparticles containing naringenin and their cytotoxicity effects in lung cancer cells. *Int J Biol Macromol* [Internet]. 2015;78:87–95. Available from: <http://dx.doi.org/10.1016/j.ijbiomac.2015.03.045>
136. Dyawanapelly S, Koli U, Dharamdasani V, Jain R, Dandekar P. Improved mucoadhesion and cell uptake of chitosan and chitosan oligosaccharide surface-modified polymer nanoparticles for mucosal delivery of proteins. *Drug Deliv Transl Res* [Internet]. 2016;6(4):365–79. Available from: <http://dx.doi.org/10.1007/s13346-016-0295-x>